Differential Contribution of Dopaminergic Transmission at D_1- and D_2-like Receptors to Cost/Benefit Evaluation for Motivation in Monkeys

Yukiko Hori[1], Yuji Nagai[1], Koki Mimura[1], Tetsuya Suhara[1], Makoto Higuchi[1], Sebastien Bouret[2] and Takafumi Minamimoto[1,*]

[1]Department of Functional Brain Imaging, National Institute of Radiological Sciences, National Institutes for Quantum and Radiological Science and Technology, Chiba, 263-8555, Japan.

[2]Team Motivation Brain & Behavior, Institut du Cerveau et de la Moelle épinière (ICM), Centre National de la Recherche Scientifique (CNRS), Hôpital Pitié Salpêtrière, 75013 Paris, France.

*Correspondence: minamimoto.takafumi@qst.go.jp (T.M.)

Abstract

It has been widely accepted that dopamine (DA) plays a major role in motivation, yet the specific contribution of DA signaling at D_1-like receptor (D_1R) and D_2-like receptor (D_2R) to cost-benefit trade-off remains unclear. Here, by combining pharmacological manipulation of DA receptors (DARs) and positron emission tomography imaging, we assessed the relationship between the degree of D_1R/D_2R blockade and changes in benefit- and cost-based motivation for goal-directed behavior of macaque monkeys. We found that the degree of blockade of either D_1R or D_2R was associated with a reduction of relative incentive effect of reward amount, where D_2R blockade had a stronger effect. Workload-discounting was selectively increased by D_2R antagonism, whereas delay-discounting was similarly increased after D_1R and D_2R blockades. These results provide fundamental insight into the specific actions of DARs in the regulation of the cost/benefit trade-off and important implications for motivational alterations in both neurological and psychiatric disorders.

Introduction

In our daily lives, we routinely determine whether to engage or disengage in an action according to its benefits and costs i.e., motivational value. For motivational value computation, the expected value of benefits (i.e., rewards) has a positive influence, while the cost necessary to earn the expected reward has a negative impact and discounts the net value of reward [1-3]. Arguably, the dopamine (DA)

system plays a central role in the benefit- and cost-based computation of motivational value. Phasic firing of midbrain DA neurons correlates with the magnitude of future rewards, while it decreases according to the expected cost to be expended for the rewards, such as physical effort, time delay to reward, and reward probability [4-9]. DA neurons are also implicated in conveying information about vigor in a sustained manner ("tonic firing"; [10, 11]). Several studies demonstrated that DA neurotransmission was causally involved in incentive motivation, i.e., in the enhancement of actions by the amount of expected reward [12-16]. In humans, the alteration of DA transmission is frequently associated with various pathological impairments of motivation such as anergia, fatigue, psychomotor retardation, and apathy, which are frequently observed in people with depression, schizophrenia or Parkinson's disease [14, 17-19]. But even if DA signaling is clearly involved in the regulation of behavior based on the cost/benefits trade-off, the underlying mechanisms remain debated.

DA signaling is mediated at post-synaptic sites by two classes of DA receptors (DARs), the D_1-like receptor (D_1R) and the D_2-like receptor (D_2R), and both classes are thought to be involved in motivation and decision-making based on the cost/benefits trade-off. For instance, blocking either D_1R or D_2R reduced the likelihood and speed of engagement of cued action to obtain a future reward [20, 21]. Blockade of either D_1R or D_2R biases animals' choices in tasks manipulating the cost/benefits trade-off, where the cost involved physical effort (effort-discounting, [22-24]) or time (delay-discounting, [23, 25]). But since in most of these studies cost and reward were not manipulated

independently, the relative impact of DA treatment on the cost vs. benefit components of evaluation remains hard to identify (see [9], for further discussion). To clarify the relation between DA, reward, and cost, it is thus critical to use behavioral task where reward and cost are manipulated independently.

Another challenge of pharmacological manipulations is how to compare the role of two receptor subtypes quantitatively. Previous studies described the effect of DAR blockade according to the antagonist dose-response relationship for each DAR subtype. However, because each antagonist has different characteristics (e.g., target affinity, brain permeability, biostability), the relationships cannot be directly compared together with the doses. On the other hand, receptor occupancy appears to provide an objective reference for receptor blockade. For example, positron emission tomography (PET) studies of patients have shown that in vivo D_2R occupancy is a reliable predictor of clinical and side effects of antipsychotic drugs [26, 27]. Similarly, receptor occupancy has been measured in rats and monkeys, and the relationship with the behavioral effects following D_2R antagonists [28-30]. Thus, to better understand the role of DARs in motivation, it would be critical to monitor occupancy following antagonists and compare the effects on distinct components of decision-making along with occupancy.

In the present study, we aimed to quantify and directly compare the roles of DA signaling via D_1R and D_2R in decision-making based on the trade-off between reward and two types of costs (time vs workload) in macaque monkeys. For this purpose, we manipulated DA transmission by

systemic application of DAR-specific antagonists and examined the relationship between the occupancy of D_1R vs D_2R and the changes in sensitivity to reward magnitude, workload and delay. We established the dynamic action of DAR antagonists by measuring the degree of DA receptor occupancy using *in vivo* PET imaging with selective radioligands. To quantify the effects of DAR blockades on incentive motivation, we used a behavioral task in which we manipulated the predicted reward size. To quantify the effects of DA manipulation on cost-based decision-making (i.e., effort or delay discounting), we used a similar behavioral task in which workload or delay to obtain a reward was manipulated. Based on our data, D_1R and D_2R have similar roles in incentive-based motivation, whereas D_2R is exclusively related to effort-based motivation.

Results

PET measurement of D_1R/D_2R occupancy following systemic antagonist administration

To establish appropriate antagonist dose setting and experimental timing, we measured the degree of receptor blockade (i.e., receptor occupancy) following systemic administration of DAR antagonists. We performed PET imaging with selective radioligands for D_1R ([^{11}C]SCH23390) and D_2R ([^{11}C]raclopride) to measure specific radioligand binding in the brain for both baseline (without drug administration) and following antagonist administration. Receptor occupancy was estimated as the degree of reduction of specific binding (S1 Fig, see methods) [31].

For D_1R measurement, high radiotracer binding was seen in the striatum at baseline condition (Fig 1A, Baseline). We used non-radiolabeled SCH23390 for D_1R antagonist at different doses (10, 30, 50, and 100 μg/kg). The striatal binding was diminished by pre-treatment with systemic administration of SCH23390 in a dose-dependent manner (Fig 1A). In 3 monkeys, we measured the relationship between D_1R occupancy and the dose of SCH23390, which was approximated by a Hill function (Fig 1C; Eq. 4). We found that treatment with SCH23390 at a dose of 100 and 30 μg/kg corresponded to 81% and 57% of D_1R occupancy, respectively.

Fig 1. D_1R and D_2R occupancy measured by PET. (A) Representative horizontal MR (left) and parametric PET images showing specific binding (BP_{ND}) of [^{11}C]SCH23390 at baseline and following drug-treatment with SCH23390 (10, 30, 50, or 100 μg/kg, i.m.). (B) Representative horizontal MR (left) and parametric PET images showing specific binding (BP_{ND}) of [^{11}C]raclopride at baseline and on 0 to 7 days after injection with haloperidol (10 μg/kg, i.m.). Color scale indicates BP_{ND} (regional binding potential relative to non-displaceable radioligand). (C) Occupancy of D_1R measured at striatal ROI is plotted against the dose of SCH23390. (D) Occupancy of D_2R measured at striatal ROI is plotted against the day after haloperidol injection. Dotted curves in C and D are the best fit of Eqs. 4 and 5, respectively.

Haloperidol was used for D_2R antagonism. Unlike SCH23390, which was rapidly washed from the brain within a few hours, a single dose of haloperidol treatment was expected to show persistent D_2R occupancy for the following several days as described in humans and mice [32, 33], providing the opportunity for testing different occupancy conditions. The baseline [^{11}C]raclopride PET image showed the highest radiotracer binding in the striatum (Fig 1B, Baseline). As expected, striatal binding was diminished not only just after pre-treatment with haloperidol (10 μg/kg, i.m.), but also until post-haloperidol day 2 (Fig 1B, *Day* 2). Binding had recovered to the baseline level by day 7 (Fig 1B, *Day 7*). We measured D_2R occupancy on days 0, 1, 2, 3, and 7 after a single haloperidol injection in 3 monkeys. An exponential decay function approximated the relationship between D_2R occupancy and post-haloperidol days (Eq. 5); a single injection of haloperidol yielded 78% and 48% of D_2R occupancy on days 0 and 1, respectively (Fig 1D).

Effects of D_1R- and D_2R-blockade on incentive motivation

To assess the effect of blockade of D_1R and D_2R on incentive motivation, we tested 2 monkeys with a reward-size task (Fig 2A). In every trial of this task, the monkeys were required to release a bar when a visual target changed from red to green to get a liquid reward. A visual cue indicated the amount of reward (1, 2, 4, or 8 drops) at the beginning of each trial (Fig 2A). After a few months of training, the monkeys were able to release the bar in response to the Go signal. However, they never performed

121 perfectly, and failures consisted of either releasing the bar too early or too late. These failures were
122 usually observed in small reward trials or close to the end of daily sessions. As in previous experiments
123 using a single option presentation which monkeys can perform correctly or not, failures were regarded
124 as trials in which the monkeys are not sufficiently motivated to correctly release the bar (i.e., refusal)
125 [2]. Hence, the frequency of refusal trials can be used as a behavioral measure of motivation [8, 34-
126 37]. Besides, we have shown that the refusal rate (E) is inversely related to reward size (R), which has
127 been formulated with a single free parameter a [2] (Fig 2B),

128 $$E = 1/aR\# \quad (1).$$

129 In agreement with these previous studies, both monkeys exhibited the inverse relationship in non-
130 treatment condition (Fig 2D and 2E, Control).

131

132 **Fig 2. D_1R/D_2R blockade increased refusal rates in reward-size task.** (A) Reward-size task. *Left:*
133 Sequence of events during a trial. *Right:* The association between visual cues and reward size. (B)
134 Schematic illustration of inverse function between refusal rate and reward size. (C) Schematic
135 illustration of two explanatory models of decrease in motivation. *Left:* Increase in refusal rate (i.e.,
136 decrease in motivation) in relation to reward size caused by decrease in incentive impact (a). *Right:*
137 An alternative model explaining increase in refusal rate irrespective of reward size. (D-E) Behavioral
138 data under D_1R and D_2R blockade, respectively. CON, control. Refusal rates (mean ± SEM) as a

function of reward size for monkeys KN (top) and ST (bottom). Dotted curves are the best-fit of inverse function (S1 Table).

We found that DAR blockade decreases incentive motivation, leading to an increase in refusal rate of the task. For example, D_1R blockade (systemic injection of SCH23390) increased the refusal rates particularly in smaller reward size trials (Fig 2D; 2-way ANOVA, treatment, $F_{(4, 19)} = 1.2$, $p < 0.05$; reward size, $F_{(3, 19)} = 105$, $p < 0.001$; interaction, $F_{(12, 19)} = 2.4$, $p < 0.05$). We considered whether this increase was due to a reduction in the incentive impact of reward, or a decrease in motivation irrespective of reward size. These factors can be captured by a decrease in parameter *a* of the inverse function and implementing intercept *e*, respectively (Fig 2C). To quantify the increases in refusal rate, we compared 4 models considering these two factors as random effects. For both monkeys, the increases in refusal rate were explained by a decrease in the parameter *a* due to the treatment, while the inverse relation with reward size was maintained (*model #3* for monkey KN and *model #1* for ST; S1 Table). We then assessed changes in parameter *a*, which indicates the incentive impact of reward size. As shown Figure 3A, normalized *a* became smaller as the dose of SCH23390 was increased to 30 or 50 μg/kg, but then it increased at the highest dose (100 μg/kg) (Fig 3A, left). Thus, incentive impact did not decrease monotonically with the dose, but changed in a U-shaped manner in both monkeys.

157

158 **Fig 3. Effect of D_1R/D_2R blockade on incentive impact of reward size.** (A) Bars indicate normalized
159 incentive impact (*a*) for each treatment condition under D_1R blockade for monkeys KN and ST. The
160 value was normalized by the value of control condition. (B) Same as A, but for D_2R blockade. (C)
161 Relationship between an incentive impact and occupancy for D_1R (blue) and D_2R blockade (red).
162 Filled circles indicate the mean of two monkeys, while individual data was plotted as triangles
163 (monkey KN) and rectangles (monkey ST), respectively.

164

165 For the D_2R blockade, the monkeys were tested with the task 15 min after a single injection
166 of haloperidol (10 μg/kg, i.m., day 0) and were then successively tested on the following days 1, 2, 3,
167 4 and 7. We also found a significant increase in refusal rates for D_2R blockades in both monkeys (Fig
168 2E). The refusal rates were highest on the day of haloperidol injection, after which they decreased as
169 the days went by (2-way ANOVA, treatment, $F_{(6, 27)} = 9.6$, $p < 0.001$). The increases in refusal rate
170 were reward size-dependent (reward size, $F_{(3, 27)} = 186$, $p < 0.001$; treatment × reward size, $F_{(18, 27)} =$
171 3.7, $p < 0.01$). Similar to the D_1R blockade, the increases in refusal rate due to D_2R blockade were
172 explained solely by a decrease of parameter *a* according to the days following the treatment for both
173 monkeys (*model* #1 for both monkeys KN and ST; S1 Table). Our model-based analysis revealed that

174 *a* decreased about 40% on the day of haloperidol injection and the following 3 days as compared to
175 control, and then recovered to almost the control level on day 7 (Fig 3B).

176 To compare the effects between D_1R and D_2R blockades directly, we plotted changes in
177 incentive impact along with the degree of blockage (Fig 3C). In both D_1R and D_2R blockades, *a*
178 declined according to the increase in occupancy; it gradually declined as D_1R occupancy increased,
179 but then increased at the highest occupancy, whereas it steeply declined until 20% D_2R occupancy,
180 and then continued to decrease slightly until 80% occupancy (Fig 3C). At 20 – 80 % occupancy, the
181 incentive impacts for D_2R blockade stayed lower than those for D_1R, suggesting a stronger sensitivity
182 of incentive impact to D_2R blockade.

183 We sought to verify that the effect of D_2R antagonism was not specific for haloperidol and
184 to validate the comparison between D_1R and D_2R in terms of receptor occupancy. We examined the
185 behavioral effect of another D_2R antagonist, raclopride, at a dose yielding about 50% receptor
186 occupancy (10 μg/kg, i.m.; S2 Fig). Following this dose of raclopride administration, a monkey again
187 exhibited increased refusal rates, which was explained by inverse function with a = 5.2 ($drop^{-1}$), a
188 comparative value of incentive impact observed at 50% D_2R occupancy with haloperidol [a = 5.4
189 ($drop^{-1}$), day 1; S2B Fig]. Thus, our data suggest that D_2R antagonism-induced reduction of the
190 incentive effect seems to reflect the degree of receptor blockade regardless of the antagonist used.
191

Effects of D_1R- and D_2R-blockade on response speed

Previous studies have reported that systemic administration of D_1R or D_2R antagonists increases reaction times (RTs) in monkeys (e.g., [38]). Consistent with those studies, DAR blockade in our study prolonged RTs in a treatment-dependent manner. For D_1R blockade, RTs were increased according to the antagonist dose (S3A and S3B Fig; 2-way ANOVA, treatment, $F_{(4, 19)} = 13.2$, $p < 0.001$), while the effect of reward size on RTs was consistent without significant interaction (reward size, $F_{(3, 19)} = 18.5$, $p < 0.001$; treatment × reward size, $F_{(12, 19)} = 0.4$, $p = 0.96$; e.g., S3C Fig). In parallel with prolonged RTs, D_1R antagonism also increased the proportion of late release (2-way ANOVA, treatment, $F_{(4, 19)} = 4.6$, $p < 0.01$; reward size, $F_{(3, 19)} = 3.0$, $p = 0.056$, treatment × reward size, $F_{(12, 19)} = 0.4$, $p = 0.94$; e.g., S3D Fig). These results suggest that D_1R blockade also influences response speed, probably due to slowing cognitive processing as implicated in previous studies [39, 40]. Thus, the effect of D_1 manipulation on value-based decision was somehow related to its effects on the action itself.

D_2R blockade also prolonged RTs, typically at days 0 and 1 (treatment, $F_{(6, 27)} = 5.6$, $p < 0.001$), while the reward size effect remained without interaction (reward size, $F_{(3, 27)} = 42$, $p < 0.001$; treatment × reward size, $F_{(18, 27)} = 0.4$, $p = 0.99$; e.g., S3E-G Fig). Prolonged RTs in 8 drop trials were limited (S3F Fig). In contrast to D_1R manipulation, D_2R blockade did not change the refusal patterns (i.e., too early or late release) (2-way ANOVA, treatment, $F_{(6, 27)} = 1.2$, $p = 0.31$; reward size, $F_{(3, 27)} = 7.6$, $p < 0.001$, treatment × reward size, $F_{(18, 27)} = 0.8$, $p = 0.68$; e.g., S3H Fig). Thus, the effect of D_2

manipulation on value-based decision was relatively independent from the effects on cognitive or motor speed itself.

Little influence of D_1R- or D_2R-blockade on internal drive or relative reward value

The behavioral data shown above suggest that blockade of DAR attenuates the incentive effect of reward on behavior. However, two important questions remain: (1) Whether the relative reward value is unaffected in general? (2) Whether the internal drive is unaffected? Previous studies in rodents showed that DA antagonism does not alter water consumption or preference for sucrose over water in rats [15, 41]. We confirmed this in primates by examining the effect of DAR blockade on water intake and sucrose preference in 2 monkeys. As expected, treatment with D_1R or D_2R antagonist did not affect overall intake (one-way ANOVA, treatment, $F_{(2, 25)} = 0.06$, $p = 0.93$) or sucrose preference (treatment, $F_{(2, 18)} = 0.70$, $p = 0.51$; S4A Fig). We also assessed blood osmolality, a physiological index of dehydration and thirst drive [42], before and after the preference test. Again, DAR treatment had no significant influence on overall osmolality or recovery of osmolality (rehydration) (2-way ANOVA, main effect of treatment, $F_{(2, 35)} = 0.08$, $p = 0.92$; treatment × pre-post, $F_{(2, 35)} = 0.15$, $p = 0.87$; S4B Fig). These results suggest that DAR blockade has no influence on physiological needs or relative reward value. These results also support the notion that the increased refusal rate was not directly due to a reduction of thirst drive.

Differential effects of D_1R and D_2R blockades on workload and delay discounting

Next, we assessed the effect of selective DAR blockade on cost-based motivation. For this purpose, we used a work/delay task (Fig 4A), where the basic features were the same as those in reward-size task. There were two trial types. In the work trials, the monkeys had to perform 0, 1, or 2 additional instrumental trials to obtain a reward. In the delay trials, after the monkeys correctly performed one instrumental trial, a reward was delivered 0–7 seconds later. The number of trials or length of delay was indicated by a visual cue presented throughout the trial. In the first trial after the reward, the visual cue informed how much would need to be paid in order to get the next reward. Therefore, we assessed the performance of the monkeys on the first trials to evaluate the impact of expected cost on motivation and decision-making. We showed that the monkeys exhibited linear relationships between refusal rate (E) and remaining costs (CU) for both work and delay trials, as follows:

$$E = kCU + E_0\# \quad (2),$$

where k is a coefficient and E_0 is an intercept [43] (Fig 4B). By extending the inference and formulation of reward-size task (Eq. 1), this linear effect proposes that the reward value is hyperbolically discounted by cost, where the coefficient k corresponds to discounting factors. Consistently, refusal rates of control condition increased as the remaining cost increased (e.g., Fig 4C, control; 2-way ANOVA, cost type × remaining cost, main effect of remaining cost, $F_{(2, 46)} = 109$, $p < 10^{-15}$). Figure

246 4B illustrates our hypothesis that DAR blockade increases cost sensitivity (i.e, discounting factor, *k*),
247 leading to an increase in refusal rate of the task.
248
249 **Fig 4. Differential effects of D_1R and D_2R blockade on cost-based motivational valuation.** (A)
250 The work/delay task. The sequence of events (left) and relationships between visual cues and trial
251 schedule in the work trials (right top 3 rows) or delay duration in the delay trials (left bottom 3 rows)
252 are shown. CU denotes the remaining (arbitrary) cost unit to get a reward, i.e., either remaining
253 workload to perform trial(s) or remaining delay periods. (B) Schematic illustration of an explanatory
254 model of increases in refusal rate by increasing cost sensitivity (*k*). (C) Effects of D_1R blockade.
255 Representative relationships between refusal rates (monkey KN; mean ± SEM) and remaining costs
256 for workload (green) and delay trials (black). Saline control (Control), moderate (30 μg/kg; MO) and
257 high D_1 occupancy treatment condition (100 μg/kg; HO) are shown. Green and black lines are the
258 best-fit lines for Eqs. 6 and 7, respectively. (D) Effects of D_2R blockade. Non-treatment control
259 (Control), moderate (1 day after haloperidol; MO) and high D_2 occupancy treatment conditions (day
260 of haloperidol; HO) are shown. Others are the same for C. (E) Comparison of effects between D_1R
261 and D_2R blockade on workload-discounting parameter (k_w). Bars and symbols indicate mean and
262 individual data, respectively. (F) Comparison of effects between D_1R and D_2R blockade on delay-
263 discounting parameter (k_d).

264

265 To compare the behavioral effect of D_1R vs D_2R antagonisms at the same degree of receptor
266 blockade, we assessed the performance of the monkeys under two comparable levels of DAR
267 occupancy for D_1R and D_2R, moderate occupancy (MO, ~50%) and high occupancy (HO, ~80%), and
268 under baseline condition (non-treatment) as a control. D_1R blockades selectively increased the refusal
269 rates in delay trials in an occupancy-dependent manner (3-way ANOVA, occupancy × cost type, $F_{(2,}$
270 $_{142)} = 5.2$, $p < 0.01$; Fig 4C). By contrast, D_2R blockade preferentially increased the refusal rates in
271 work trials (occupancy × cost type, $F_{(2, 142)} = 25$, $p < 10^{-9}$; Fig 4D). Like our previous study [43], two
272 linear regression models (Eqs. 6 and 7, see methods) simultaneously fitted the data well in all cases
273 (average $R^2 > 0.9$), allowing us to measure the effects of DAR as the increased steepness of cost-
274 discounting of motivational value. We found that workload-discounting (k_w) was specifically
275 increased by D_2R blockade in an occupancy-dependent manner (2-way ANOVA, receptor subtype ×
276 occupancy, $F_{(2, 10)} = 14.1$, $p < 0.01$; Fig 4E). Delay-discounting, on the other hand, was inclined to
277 increase according to the degree of DAR blockade irrespective of receptor subtype (main effect of
278 occupancy, $F_{(2, 10)} = 4.0$, $p = 0.054$; receptor subtype × occupancy, $F_{(2, 10)} = 0.3$, $p = 0.74$; Fig 4F).

279 In line with what we found in the reward-size task, D_1R blockade significantly increased the
280 proportion of late release (3-way ANOVA, main effect of treatment, $F_{(2, 34)} = 9.0$, $p < 0.001$), whereas
281 D_2R blockade did not (main effect of treatment, $F_{(2, 33)} = 0.3$, $p = 0.73$). The frequency of touching and

282 releasing the bar during delay periods — actions that have no instrumental role in delay trials — was
283 also unaffected (2-way ANOVA, treatment × delay duration; treatment; D_1R, $F_{(2, 10)} = 2.1$, $p = 0.16$;
284 D_2R, $F_{(2, 10)} = 1.9$, $p = 0.21$). Thus, D_1R blockade also affects the response itself in the work/delay task
285 in addition to increases in cost-discounting.

286 Considering the direct and indirect striatal output pathways where neurons exclusively
287 express D_1R and D_2R, respectively, and the opposition believed to exist between the pathways in
288 general, it should be possible to counterbalance the effects of those antagonists with each other [44].
289 To test this possibility, we examined the behavioral effects of both D_1R and D_2R blockades at the same
290 occupancy level. After treatment with both SCH23390 (100 μg/kg) and haloperidol (10 μg/kg),
291 seemingly achieving ~80% of occupancy for both subtypes (cf. Fig 1C and 1D), all monkeys stopped
292 performing the task with a small number of correct trials (1-13% of control). When we treated the
293 monkeys with SCH23390 (30 μg/kg) on the day following that of haloperidol injection (i.e., both D_1R
294 and D_2R assumed to be occupied at ~50%), the monkeys had higher refusal rates in delay trials than
295 control (Fig 5A, D_1R+D_2R block) and displayed a higher discounting factor (Fig 5B, delay). By
296 contrast, this simultaneous D_1R and D_2R blockade appeared to attenuate the effect of D_2R antagonism
297 on workload in 2 of 3 monkeys; the refusal rates in work trials were not as high as in D_2R blockade
298 alone (Fig 5A), and the workload-discounting factor (k_w) became the value between that for D_1 and
299 D_2 antagonisms (Fig 5B, workload). A similar counterbalance was also seen in the relative strength of

300 discounting (ratio of k_w / k_d) as well as the motivation for the minimum cost trials (E_0) (Fig 5B). These
301 results suggest that blocking both receptor subtypes tends to induce a synergistic effect on delay-
302 discounting, while it compensates the effects on workload-discounting.
303
304 **Fig 5. Effect of both D_1R and D_2R blockades on cost evaluation for motivation.** (A) Representative
305 relationship between refusal rates (in monkey KN; mean ± SEM) and remaining costs for workload
306 (green) and delay trials (black). (B) Best-fit parameters, workload-discounting (k_w), delay-discounting
307 (k_d), workload/delay ratio (k_w/k_d), and intercept (E_0), are plotted for each treatment condition. Bars and
308 symbols indicate mean and individual data, respectively. D_1R+D_2R block indicates the data obtained
309 under both D_1R and D_2R blockades at moderate occupancy, while D_1R and D_2R blockades at high
310 occupancy resulted in almost no correct performance (see text). All parameters are derived from the
311 best fit for Eqs. 6 and 7, respectively.
312
313 **Discussion**
314 Combining the PET occupancy study and pharmacological manipulation of D_1- and D_2-like receptors
315 with quantitative measurement of motivation in monkeys, the current study demonstrated dissociable
316 roles of the DA transmissions via D_1R and D_2R in the computation of the cost/benefits trade-off to
317 guide action. To the best of our knowledge, this is the first study to directly compare the contribution

318 of dopamine D_1R and D_2R along with the degree of receptor blockade. Using model-based analysis,
319 we showed that DAR blockade had a clear quantitative effect on the sensitivity of animals to
320 information about potential costs and benefits, without any qualitative effect on the way monkeys
321 integrated costs and benefits and adjusted their behavior. We showed that blockade of D_1R or D_2R
322 reduced the incentive impact of reward as the degree of DAR blockade increased, and the incentive
323 impact was more sensitive to the D_2R blockade than the D_1R blockade at lower occupancy. In cost-
324 discounting experiments, we could dissociate the relation between each DAR type and workload vs
325 delay-discounting: workload-discounting was increased exclusively by D_2R antagonism, whereas
326 delay-discounting was increased by DAR blockade irrespective of receptor subtype. When both D_1R
327 and D_2R were blocked simultaneously, the effects were synergistic and strengthened for delay-
328 discounting, while the effects were antagonistic and diminished for workload-discounting.
329
330 *DA controls the incentive effect of expected reward amount*
331 Previous pharmacological studies have shown that DAR blockade decreased the speed of action and/or
332 probability of engagement behavior [20, 21]. However, the previous studies did not address the
333 quantitative effect of DAR blockade on incentive motivation; more specifically, there was a lack of
334 experimental data to model the causal relationship among DAR stimulation, reward, and motivation.
335 In the present study, we used a behavioral paradigm that enabled us to formulate and quantify the

relationship between reward and motivation [2] (Fig 2). Our finding, a reduction of incentive impact due to DAR antagonism (cf., Fig 3) is in line with the incentive salience theory, that is, DA transmission attributes salience to incentive cue to promote goal-directed action [12]. The lack of effect of DA manipulation on satiety and spontaneous water consumption are compatible with the idea that DA manipulation has a stronger effect on incentive processes (influence of reward on action) than on hedonic processes (evaluation itself, pleasure associated with consuming reward), but further experiments would be necessary to address that point directly [12].

Our model-based analysis indicates that DAR blockade only had a quantitative influence (a reduction of incentive impact of reward) without changing the qualitative relationship between reward size and behavior. This is in marked contrast with the reported effects of inactivation of brain areas receiving massive DA inputs, including the orbitofrontal cortex, rostromedial caudate nucleus, and ventral pallidum. Indeed, in experiments using nearly identical tasks and analysis, inactivation or ablation of these regions produced a qualitative change in the relationship between reward size and behavior (more specifically, a violation of the inverse relationship between reward size and refusal rates) [36, 37, 45]. Thus, the influence of DAR cannot be understood as a simple permissive or activating effect on target regions. The specificity of the DAR functional role is further supported by the subtle, but significant difference between the behavioral consequences of blocking of D_1R vs D_2R. By combining a direct measure of DAR occupancy and quantitative behavioral assessment, the present

study demonstrates that the incentive impact of reward is more sensitive to D_2R blockade than D_1R blockade, and especially at a lower degree of occupancy (cf. Fig 3C). Moreover, the dose-response relation between occupancy and behavior was monotonous for D_2R, but U-shaped for D_1R. Although this might be surprising, such non-monotonic effects have been repeatedly reported. For example, working memory performance and related neural activity in the prefrontal cortex takes the form of an "inverted-U" shaped curve, where too little or too much D_1R activation impairs cognitive performance [3, 46, 47]. As for the mechanisms underlying the distinct functional relation between the behavioral effects of D_1R vs D_2R blockade, it is tempting to speculate that this is related to a difference in their distribution, their affinity and the resulting relation with phasic vs tonic DA action. Indeed, DA affinity for D_2R is ~100 times higher than that for D_1R [48]. This is directly in line with the higher behavioral sensitivity of D_2R manipulation, compared to that of D_1R. Moreover, in the striatum, a basal DA concentration of ~5–10 nM is sufficient to constantly stimulate D_2R. Using available biological data, a recent simulation study showed that the striatal DA concentration produced by the tonic activity of DA neurons (~40 nM) would occupy 75% of D_2R but only 3.5% of D_1R [49]. Thus, blockade of D_2R at low occupancy may interfere with tonic DA signaling, whereas D_1R occupancy would only be related to phasic DA action, i.e., when transient but massive DA release occurs (e.g., in response to critical information about reward). We acknowledge that this remains very hypothetical, but

371 irrespective of the underlying mechanisms, our data clearly support the idea that DA action on D_1R vs
372 D_2R exerts distinct actions on their multiple targets to enhance incentive motivation.
373
374 *DA transmission via D_1R and D_2R distinctively controls cost-based motivational process*
375 Although many rodent studies have demonstrated that attenuation of DA transmission alters not only
376 benefit- but also cost-related decision-making, the exact contribution of D_1R and D_2R remains elusive.
377 For example, reduced willingness to exert physical effort to receive higher reward was similarly found
378 following D_1 and D_2 antagonisms in some studies, while it was observed exclusively by D_2 antagonism
379 in other studies [22, 50, 51]. This inconsistency may arise because previous studies usually
380 investigated the effect of antagonism on D_1R and D_2R along with a relative pharmacological
381 concentration (e.g., low and high doses). In the present study, PET-assessed DAR manipulation
382 allowed us to directly compare the behavioral effect between D_1R and D_2R with an objective reference,
383 namely occupancy (i.e., ~50% and ~80% occupancy). Besides, the exact nature of the cost (effort vs
384 delay) has sometimes been difficult to identify, and effort manipulation is often strongly correlated
385 with reward manipulation (typically when the amount of reward earned is instrumentally related to the
386 amount of effort exerted, see [9]). Here, using a task manipulating forthcoming workload
387 independently from reward value, we demonstrated that blockade of D_2R, but not D_1R, increased
388 workload-discounting in an occupancy-dependent manner while maintaining linearity (*cf.*, Fig 4E). In

addition, D_1R and D_2R had synergistic effects in the delay-discounting tasks but antagonistic effects in the workload-discounting task, which also indicates that the DAR contribution to delay- vs workload-discounting is qualitatively different. Thus, even if workload trials also include a delay component in our task, the distinct effects of DAR manipulations confirm that the nature of the cost in the workload and delay trials differs, at least from a neurobiological point of view [43]. Thus, these results extend previous studies demonstrating increased effort-discounting by D_2R blockade [23, 52] and support the notion that DA activation allows overcoming effort costs through a mechanism that can be distinguished from that of incentive motivation, which involves both D_1R and D_2R.

Delay-discounting and impulsivity — the tendency associated with excessive delay-discounting — are also thought to be linked to the DA system [53, 54]. Systemic administration of D_1R or D_2R antagonist increases preference for immediate small rewards, rather than larger and delayed rewards [23, 25, 55, 56]. Concurrently, some of these studies also showed negative effects of D_1R [25] or D_2R blockade [56] on impulsivity. These inconsistencies may be attributed to the differences in behavioral paradigms or drugs (and doses) used. Our PET-assessed DAR manipulation demonstrated that blockade of D_1R and D_2R at the same occupancy level (~50% and ~80%) similarly increased delay-discounting (Fig 4F), suggesting that DA transmission continuously adjusts delay-discounting at the post-synaptic site. This observation is in good accord with the previous finding that increasing DA transmission decreases temporal discounting; e.g., amphetamine or methylphenidate

increased the tendency to choose long-delays options for larger rewards [25, 55-58]. In contrast with workload-discounting, however, the relation with DAR in delay-discounting and incentive-motivation could not be distinguished, in that both D_1R and D_2R might be involved. This is reminiscent of neurophysiological data, revealing that DA neurons show a strong sensitivity to both reward and delay, but a weaker sensitivity to effort [8, 59, 60]. Altogether, this is in line with the notion that the DA system does not process upcoming benefits (information about potential benefits, including their distribution in space and time) in the same way it processes upcoming costs (here defined as energy expenditure) [9].

This differential relation between DA and delay vs workload might be related to the differential expression of these receptors in the direct vs indirect striatopallidal pathway, where the striatal neurons exclusively express D_1R and D_2R, respectively [61]. Opposing functions between these pathways have been proposed: activity of the direct pathway (D_1R) neurons reflects positive rewarding events promoting movement, whereas activity of the indirect pathway (D_2R) neurons is related to negative values mediating aversion or inhibiting movements [44, 62] (but see [63]). DA increases the excitability of direct-pathway neurons, and this effect was reduced by D_1R antagonism, decreasing motor output. DA reduces the responsiveness of indirect pathway neurons via D_2R [61], and blockade of D_2R would increase the activity, reducing motor output via decreased thalamocortical drive [64]. This scenario may explain our finding of a synergistic effect of simultaneous D_1R and D_2R

425 blockade on delay-discounting (*cf.* Fig 5). Further work would be necessary to clarify this hypothesis,
426 including the dynamic relation with tonic vs phasic DA release, but altogether, these data strongly
427 support the idea that the distinct contribution of the DA system to benefits (reward availability) and
428 costs (energy expenditure) involves a complementary action of the direct and indirect pathways.
429
430 *Limitations of the current study*
431 Finally, the limitations of the current study and areas for further research can be discussed. First,
432 because of applying systemic antagonist administration, the current study could not determine which
433 brain area(s) is responsible for antagonist-induced alterations of benefit- and cost-based motivation.
434 While our data support the idea that differential neural networks involve workload- and delay-
435 discounting, further study (e.g., local infusion of DA antagonist) is needed to identify the locus of the
436 effects, generalizing our findings to unravel the circuit and molecular mechanism of motivation. We
437 should also note that the current study does not address dynamic learning paradigms and therefore
438 does not generalize our findings to the function of the DA system in learning directly. Despite these
439 limitations, the current study provides unique insights into the role of the DA system in the
440 motivational process.
441
442 *Conclusion*

443 In summary, the present study demonstrates an apparent dissociation of the functional role of DA
444 transmission via D_1- and D_2-like receptors in benefit- and cost-based motivational processing. DA
445 transmissions via D_1R and D_2R modulate both the incentive impact of reward size and the negative
446 influence of delay. By contrast, workload-discounting is regulated exclusively via D_2R. In addition,
447 D_1R and D_2R had synergistic effects on delay-discounting but opposite effects on workload-
448 discounting. These dissociations can be attributed to differential involvement of the direct and indirect
449 striatofugal pathways in workload- and delay-discounting. Together, our findings add an important
450 aspect to our current knowledge concerning the role of DA signaling motivation based on the trade-
451 off between costs and benefits, thus providing an advanced framework for understanding the
452 pathophysiology of psychiatric disorders.
453

454 **Materials and Methods**

455 **Ethics statement**

456 All surgical and experimental procedures were approved by the Animal Care and Use Committee of
457 the National Institutes for Quantum and Radiological Science and Technology (#09-1035), and were
458 in accordance with the Institute of Laboratory Animal Research *Guide for the Care and Use of*
459 *Laboratory Animals*.
460

461 **Subjects**

462 A total of nine male adult macaque monkeys (8 Rhesus and 1 Japanese; 4.6-7.7 kg) were used in this
463 study. Food was available ad libitum, and motivation was controlled by restricting access to fluid to
464 experimental sessions, when water was delivered as a reward for performing the task. Animals
465 received water supplementation whenever necessary (e.g., if they could not obtain enough water
466 through experiments), and they had free access to water whenever testing was interrupted for more
467 than a week.

468

469 **Drug treatment**

470 All experiments in this study were carried out with injected intramuscular (i.m.) SCH23390 (Sigma-
471 Aldrich), haloperidol (Dainippon Sumitomo Pharma, Japan), and raclopride (Sigma-Aldrich)
472 dissolved or diluted in 0.9% saline solution. Animals were pretreated with an injection of SCH23390
473 (10, 30, 50, or 100 μg/kg), haloperidol (10 μg/kg), or raclopride (10 or 30 μg/kg) 15 min before the
474 beginning of the behavioral testing or PET scan. In behavioral testing, saline was injected as a vehicle
475 control by the same procedure as drug treatment. The administered volume was 1 mL across all
476 experiments with each monkey.

477

478 **PET procedure and occupancy measurement**

Four monkeys were used in the measurement. PET measurements were performed with two PET ligands: [^{11}C]SCH23390 (for studying D_1R binding) and [^{11}C]raclopride (for studying D_2R binding). The injected radioactivities of [^{11}C]SCH23390 and [^{11}C]raclopride were 91.7 ± 6.0 MBq (mean ± SD) and 87.0 ± 4.9 MBq, respectively. Specific radioactivities of [^{11}C]SCH23390 and [^{11}C]raclopride at the time of injection were 86.2 ± 40.6 GBq/μmol and 138.2 ± 70.1 GBq/μmol, respectively. All PET scans were performed using an SHR-7700 PET scanner (Hamamatsu Photonics Inc., Japan) under conscious conditions and seated in a chair. Prior to the PET study, the monkeys underwent surgery to implant a head-hold device using aseptic techniques [65]. After transmission scans for attenuation correction using a ^{68}Ge–^{68}Ga source, a dynamic scan in three-dimensional (3D) acquisition mode was performed for 60 min ([^{11}C]SCH23390) or 90 min ([^{11}C]raclopride). The ligands were injected via crural vein as a single bolus at the start of the scan. All emission data were reconstructed with a 4.0-mm Colsher filter. Tissue radioactive concentrations were obtained from volumes of interest (VOIs) placed on several brain regions where DARs are relatively abundant: caudate nucleus, putamen, nucleus accumbens (NAcc), thalamus, hippocampus, amygdala, parietal cortex, principal sulcus (PS), dorsolateral prefrontal cortex (dlPFC), and ventrolateral prefrontal cortex (vlPFC), as well as the cerebellum (as reference region). Each VOI was defined on individual T1-weighted axial magnetic resonance (MR) images (EXCELART/VG Pianissimo at 1.0 tesla, Toshiba, Japan) that were co-registered with PET images using PMOD® image analysis software (PMOD Technologies Ltd,

497 Switzerland). Regional radioactivity of each VOI was calculated for each frame and plotted against
498 time. Regional binding potentials relative to non-displaceable radioligands (BP_{ND}) of D_1R and D_2R
499 were estimated with a simplified reference tissue model on VOI and voxel-by-voxel bases [66-68].
500 The monkeys were scanned with and without drug-treatment condition on different days.

501 Occupancy levels were determined from the degree of reduction (%) of BP_{ND} by antagonists [69].
502 DA receptor occupancy was estimated as follows:

503 $$Occupancy(\%) = (1 - BP_{NDTreatment}/BP_{NDBaseline}) \times 100 \quad (3),$$

504 where $BP_{ND\ Baseline}$ and $BP_{ND\ Treatment}$ are BP_{ND} measured without (baseline) and with an antagonist,
505 respectively. Relationship between D_1R occupancy (D_1 Occ) and dose of SCH23390 (Dose) was
506 estimated with 50% effective dose (ED_{50}) as follows:

507 $$D_1Occ(\%) = 100 \times Dose/(ED50 + Dose)\# \quad (4).$$

508 Relationship between D_2R occupancy (D_2 Occ) and days after haloperidol injection was estimated
509 using the level at day 0 with a decay constant (λ) as follows:

510 $$D_2Occ(\%) = Occ_{Day0}e^{-\lambda Day} \quad (5).$$

511

512 **Behavioral tasks and testing procedures**

513 Three monkeys (ST, 6.4 kg; KN, 6.3 kg; M7, 7.3 kg) were used for the behavioral study. For all
514 behavioral training and testing, each monkey sat in a primate chair inside a sound-attenuated dark

515 room. Visual stimuli were presented on a computer video monitor in front of the monkey. Behavioral
516 control and data acquisition were performed using the REX program. Neurobehavioral Systems
517 Presentation software was used to display visual stimuli (Neurobehavioral Systems). We used two
518 types of behavioral tasks, *reward-size task* and *work/delay task*, as described previously [2, 43]. Both
519 tasks consisted of color discrimination trials (see Figs 2A and 4A). Each trial began when the monkey
520 touched a bar mounted at the front of the chair. The monkey was required to release the bar between
521 200 and 1,000 ms after a red spot (wait signal) turned green (go signal). On correctly performed trials,
522 the spot then turned blue (correct signal). A visual cue was presented at the beginning of each color
523 discrimination trial (500 ms before the red spot appearing).

524 In the reward-size task, a reward of 1, 2, 4, or 8 drops of water (1 drop = ~0.1 mL) was delivered
525 immediately after the blue signal. Each reward size was selected randomly with equal probability. The
526 visual cue presented at the beginning of the trial indicated the number of drops for the reward (Fig
527 2A).

528 In the work/delay task, a water reward (~0.25 mL) was delivered after each correct signal
529 immediately or after an additional 1 or 2 instrumental trials (work trial), or after a delay period (delay
530 trials). The visual cue indicated the combination of the trial type and requirement to obtain a reward
531 (Fig 4A). Pattern cues indicated the delay trials with the timing of reward delivery after a correct
532 performance: either immediately (0.3 s, 0.2 – 0.4 s; mean, range), a short delay (3.6 s, 3.0 – 4.2 s), or

a long delay (7.2 s, 6.0 – 8.4 s). Grayscale cues indicated work trials with the number of trials the monkey would have to perform to obtain a reward. We set the delay durations to be equivalent to the duration for 1 or 2 trials of color discrimination trials, so that we could directly compare the cost of 1 or 2 arbitrary units (cost unit; CU).

If the monkey released the bar before the green target appeared or within 200 ms after the green target appeared or failed to respond within 1 s after the green target appeared, we regarded the trial as a "refusal trial"; all visual stimuli disappeared, the trial was terminated immediately, and after the 1-s inter-trial interval, the trial was repeated. Our behavioral measurement for the motivational value of outcome was the proportion of refusal trials. Before each testing session, the monkeys were subject to ~22 hours of water restriction in their home cage. Each session continued until the monkey would no longer initiate a new trial (usually less than 100 min).

Before this experiment, all monkeys had been trained to perform color discrimination trials in the cued multi-trial reward schedule task for more than 3 months. The monkeys were tested with the work/delay task for 1-2 daily sessions as training to become familiar with the cueing condition.

Each monkey was tested from Monday to Friday. Treatment with SCH23390 was performed every four or five days. On other days without SCH23390, sessions with saline (1 mL) treatment were analyzed as control sessions. Haloperidol was given every two or three weeks on Monday or Tuesday, because D_2R occupancy persisted for several days after a single dose of haloperidol treatment (Fig

1D). The days before haloperidol treatment were analyzed as control sessions. Each dose of SCH23390 or a single dose of haloperidol was tested 4 or 5 times per each animal.

Sucrose preference test

Two monkeys (RO, 5.8kg; KY, 5.6kg) were used for the sucrose preference test. The test was performed in their home cages once a week. In advance of the test, water access was prevented for 22 h. The monkeys were injected with SCH23390 (30 μg/kg), haloperidol (10 μg/kg), or saline 15 min before the sucrose preference test. Two bottles containing either 1.5% sucrose solution or tap water were set into bottle holders in the home cage and the monkeys were allowed to freely consume fluids for 2h. The total amount of sucrose (SW) and tap water (TW) intake was measured and calculated as sucrose preference index (SP) as follows: SP = (SW – TW) / (SW + TW). The position of sucrose and tap water bottles (right or left toward the front panel of the home cage) was counterbalanced across sessions and monkeys. Drugs or saline was injected alternatively once a week. We also measured the osmolality level in blood samples (1 mL) obtained immediately before and after each testing session.

Behavioral data analysis

All data and statistical analyses were performed using the R statistical computing environment (R Development Core Team, 2004). The average error rate for each trial type was calculated for each

daily session, with the error rates in each trial type being defined as the number of error trials divided by the total number of trials of that given type. The monkeys sometimes made many errors at the beginning of the daily session, probably due to high motivation/impatience; we excluded the data until the 1st successful trial in these cases. A trial was considered an error trial if the monkey released the bar either before or within 200 ms after the appearance of the green target (early release) or failed to respond within 1 s after the green target (late release). We did not distinguish between the two types of errors and used their sum except for the error pattern analysis. We performed repeated-measures ANOVAs to test the effect of treatment × reward size (for the data in reward-size task) or treatment × cost type × remaining cost (for the data in work/delay task) on error rate, on late release rate (i.e., error pattern), on reaction time, and on movements during the delay.

We used the refusal rates to estimate the level of motivation because the refusal rates of these tasks (E) are inversely related to the value for action [2]. In the reward-size task, we used the inverse function (Eq. 1). We fitted the data to linear mixed models [70], in which the random effects across DAR blockade conditions on parameter a and/or intercept e (Fig 2C) were nested. Model selection was based on Akaike's information criterion (AIC), an estimator of in-sample prediction error for the nested models (S1 Table). Using the selected model, the parameter a was estimated individually, and then normalized by the value in non-treated condition (CON) (Fig 3A and 3B).

In the work/delay task, we used linear models to estimate the effect of remaining cost, i.e., workloads and delay, as described previously [43],

$$E_w = k_w CU + E_0 \quad (6),$$

$$E_d = k_d CU + E_0 \quad (7),$$

where E_w and E_d are the error rates, and k_w and k_d are cost factors for work and delay trials, respectively. CU is the number of remaining cost units, and E_0 is the intercept. We simultaneously fitted a pair of these linear models to the data by sum-of-squares minimization without weighting. The coefficient of determination (R^2) was reported as a measure of goodness of fit.

Acknowledgements

We thank R. Suma, T. Okauchi, Y. Sugii, R. Yamaguchi, Y. Matsuda, and J. Kamei for their technical assistance, and K. Oyama for discussion. We also thank to Dr. M-R. Zhang and his colleagues at Department of Radiopharmaceuticals Development, NIRS/QST for producing the radioligands. A Japanese monkey used in this study was provided by National Bio-Resource Project "Japanese Monkeys" of the MEXT, Japan.

References

603 1. Berridge KC. Motivation concepts in behavioral neuroscience. Physiol Behav. 2004;81(2):179-
604 209. doi: 10.1016/j.physbeh.2004.02.004.
605 2. Minamimoto T, La Camera G, Richmond BJ. Measuring and modeling the interaction among
606 reward size, delay to reward, and satiation level on motivation in monkeys. J Neurophysiol.
607 2009;101(1):437-47. doi: 10.1152/jn.90959.2008.
608 3. Zahrt J, Taylor JR, Mathew RG, Arnsten AF. Supranormal stimulation of D1 dopamine receptors
609 in the rodent prefrontal cortex impairs spatial working memory performance. J Neurosci.
610 1997;17(21):8528-35. doi: 10.1523/jneurosci.17-21-08528.
611 4. Fiorillo CD, Tobler PN, Schultz W. Discrete coding of reward probability and uncertainty by
612 dopamine neurons. Science. 2003;299(5614):1898-902. doi: 10.1126/science.1077349.
613 5. Kobayashi S, Schultz W. Influence of reward delays on responses of dopamine neurons. J Neurosci.
614 2008;28(31):7837-46. doi: 10.1523/jneurosci.1600-08.2008.
615 6. Ravel S, Richmond BJ. Dopamine neuronal responses in monkeys performing visually cued
616 reward schedules. Eur J Neurosci. 2006;24(1):277-90. doi: 10.1111/j.1460-9568.2006.04905.x.
617 7. Tobler PN, Fiorillo CD, Schultz W. Adaptive coding of reward value by dopamine neurons.
618 Science. 2005;307(5715):1642-5. doi: 10.1126/science.

8. Varazzani C, San-Galli A, Gilardeau S, Bouret S. Noradrenaline and Dopamine Neurons in the Reward/Effort Trade-Off: A Direct Electrophysiological Comparison in Behaving Monkeys. J Neurosci. 2015;35(20):7866-77. doi: 10.1523/ jneurosci.0454-15.2015.

9. Walton ME, Bouret S. What Is the Relationship between Dopamine and Effort? Trends Neurosci. 2019;42(2):79-91. doi: 10.1016/j.tins.2018.10.001.

10. Cools R, Nakamura K, Daw ND. Serotonin and dopamine: unifying affective, activational, and decision functions. Neuropsychopharmacology. 2011;36(1):98-113. doi: 10.1038/npp.2010.121.

11. Niv Y, Joel D, Dayan P. A normative perspective on motivation. Trends Cogn Sci. 2006;10(8):375-81. doi: 10.1016/j.tics.2006.06.010.

12. Berridge KC. The debate over dopamine's role in reward: the case for incentive salience. Psychopharmacology (Berl). 2007;191(3):391-431. doi: 10.1007/s00213-006-0578-x.

13. Le Bouc R, Rigoux L, Schmidt L, Degos B, Welter ML, Vidailhet M, et al. Computational Dissection of Dopamine Motor and Motivational Functions in Humans. J Neurosci. 2016;36(25):6623-33. doi: 10.1523/jneurosci.3078-15.2016.

14. Muhammed K, Manohar S, Ben Yehuda M, Chong TT, Tofaris G, Lennox G, et al. Reward sensitivity deficits modulated by dopamine are associated with apathy in Parkinson's disease. Brain. 2016;139(Pt 10):2706-21. doi: 10.1093/brain/aww188.

636 15. Salamone JD, Correa M. Motivational views of reinforcement: implications for understanding the
637 behavioral functions of nucleus accumbens dopamine. Behav Brain Res. 2002;137(1-2):3-25. doi:
638 10.1016/s0166-4328(02)00282-6.
639 16. Walton ME, Kennerley SW, Bannerman DM, Phillips PE, Rushworth MF. Weighing up the
640 benefits of work: behavioral and neural analyses of effort-related decision making. Neural Netw.
641 2006;19(8):1302-14. doi: 10.1016/j.neunet.2006.03.005.
642 17. Buyukdura JS, McClintock SM, Croarkin PE. Psychomotor retardation in depression: Biological
643 underpinnings, measurement, and treatment. Prog Neuro-Psychoph. 2011;35(2):395-409. doi:
644 10.1016/j.pnpbp.2010.10.019.
645 18. Demyttenaere K, De Fruyt J, Stahl SM. The many faces of fatigue in major depressive disorder.
646 Int J Neuropsychoph. 2005;8(1):93-105. doi: 10.1017/S1461145704004729.
647 19. Salamone JD, Yohn SE, Lopez-Cruz L, San Miguel N, Correa M. Activational and effort-related
648 aspects of motivation: neural mechanisms and implications for psychopathology. Brain.
649 2016;139(Pt 5):1325-47. doi: 10.1093/brain/aww050.
650 20. Choi WY, Morvan C, Balsam PD, Horvitz JC. Dopamine D1 and D2 Antagonist Effects on
651 Response Likelihood and Duration. Behav Neurosci. 2009;123(6):1279-87.
652 doi:10.1037/a0017702

653 21. Pattij T, Janssen MC, Vanderschuren LJ, Schoffelmeer AN, van Gaalen MM. Involvement of
654 dopamine D1 and D2 receptors in the nucleus accumbens core and shell in inhibitory response
655 control. Psychopharmacology (Berl). 2007;191(3):587-98. doi: 10.1007/s00213-006-0533-x.
656 22. Bardgett ME, Depenbrock M, Downs N, Points M, Green L. Dopamine Modulates Effort-Based
657 Decision Making in Rats. Behav Neurosci. 2009;123(2):242-51. doi: 10.1037/a0014625.
658 23. Denk F, Walton ME, Jennings KA, Sharp T, Rushworth MF, Bannerman DM. Differential
659 involvement of serotonin and dopamine systems in cost-benefit decisions about delay or effort.
660 Psychopharmacology (Berl). 2005;179(3):587-96. doi: 10.1007/s00213-004-2059-4.
661 24. Salamone JD. Dopamine, effort, and decision making: theoretical comment on Bardgett et al.
662 (2009). Behav Neurosci. 2009;123(2):463-7. doi: 10.1037/a0015381.
663 25. Wade TR, de Wit H, Richards JB. Effects of dopaminergic drugs on delayed reward as a measure
664 of impulsive behavior in rats. Psychopharmacology. 2000;150(1):90-101.
665 doi:10.1007/s002130000402.
666 26. Farde L, Nordström A, Wiesel F, Pauli S, Halldin C, Sedvall G. Positron emission tomographic
667 analysis of central D1 and D2 dopamine receptor occupancy in patients treated with classical
668 neuroleptics and clozapine. Relation to extrapyramidal side effects. Archives of general psychiatry.
669 1992;49(7):538. doi:10.1001/archpsyc.1992.01820070032005.

670 27. Kapur S, Zipursky R, Jones C, Remington G, Houle S. Relationship between dopamine D(2)
671 occupancy, clinical response, and side effects: a double-blind PET study of first-episode
672 schizophrenia. Am J Psychiatry. 2000;157(4):514-20. doi: 10.1176/appi.ajp.157.4.514.
673 28. Takano A, Suhara T, Maeda J, Ando K, Okauchi T, Obayashi S, et al. Relation between cortical
674 dopamine D(2) receptor occupancy and suppression of conditioned avoidance response in non-
675 human primate. Psychiatry Clin Neurosci. 2004;58(3):330-2. doi: 10.1111/j.1440-
676 1819.2004.01240.x.
677 29. Wadenberg ML, Kapur S, Soliman A, Jones C, Vaccarino F. Dopamine D2 receptor occupancy
678 predicts catalepsy and the suppression of conditioned avoidance response behavior in rats.
679 Psychopharmacology (Berl). 2000;150(4):422-9. doi: 10.1007/s002130000466.
680 30. Wadenberg ML, Soliman A, VanderSpek SC, Kapur S. Dopamine D(2) receptor occupancy is a
681 common mechanism underlying animal models of antipsychotics and their clinical effects.
682 Neuropsychopharmacology. 2001;25(5):633-41. doi: 10.1016/S0893-133X(01)00261-5.
683 31. Halldin C, Gulyas B, Farde L. PET studies with carbon-11 radioligands in
684 neuropsychopharmacological drug development. Curr Pharm Des. 2001;7(18):1907-29. doi:
685 10.2174/1381612013396871.

686 32. Ishiwata K, Kawamura K, Kobayashi T, Matsuno K. Sigma1 and dopamine D2 receptor occupancy
687 in the mouse brain after a single administration of haloperidol and two dopamine D2-like receptor
688 ligands. Nucl Med Biol. 2003;30(4):429-34. doi: 10.1016/s0969-8051(03)00003-9.
689 33. Nordstrom AL, Farde L, Halldin C. Time course of D2-dopamine receptor occupancy examined
690 by PET after single oral doses of haloperidol. Psychopharmacology (Berl). 1992;106(4):433-8.
691 doi: 10.1007/bf02244811.
692 34. Bouret S, Richmond BJ. Sensitivity of locus ceruleus neurons to reward value for goal-directed
693 actions. J Neurosci. 2015;35(9):4005-14. doi: 10.1523/jneurosci.4553-14.2015.
694 35. Eldridge MA, Lerchner W, Saunders RC, Kaneko H, Krausz KW, Gonzalez FJ, et al.
695 Chemogenetic disconnection of monkey orbitofrontal and rhinal cortex reversibly disrupts reward
696 value. Nat Neurosci. 2016;19(1):37-9. doi: 10.1038/nn.4192.
697 36. Fujimoto A, Hori Y, Nagai Y, Kikuchi E, Oyama K, Suhara T, et al. Signaling Incentive and Drive
698 in the Primate Ventral Pallidum for Motivational Control of Goal-Directed Action. J Neurosci.
699 2019;39(10):1793-804. doi: 10.1523/jneurosci.2399-18.2018.
700 37. Nagai YJ, Kikuchi E, Lerchner W, Inoue K, Ji B, Eldridge MAG, et al. PET imaging-guided
701 chemogenetic silencing reveals a critical role of primate rostromedial caudate in reward evaluation.
702 Nat Commun. 2016;7:13605. doi:10.1038/ncomms13605.

703 38. Weed MR, Gold LH. The effects of dopaminergic agents on reaction time in rhesus monkeys.
704 Psychopharmacology (Berl). 1998;137(1):33-42. doi: 10.1007/s002130050590.
705 39. Muller U, von Cramon DY, Pollmann S. D1- versus D2-receptor modulation of visuospatial
706 working memory in humans. J Neurosci. 1998;18(7):2720-8. doi:10.1523/jneurosci.18-07-02720.
707 40. Sawaguchi T, Goldman-Rakic PS. D1 dopamine receptors in prefrontal cortex: involvement in
708 working memory. Science. 1991;251(4996):947-50. doi: 10.1126/science.1825731.
709 41. Salamone JD, Steinpreis RE, McCullough LD, Smith P, Grebel D, Mahan K. Haloperidol and
710 nucleus accumbens dopamine depletion suppress lever pressing for food but increase free food
711 consumption in a novel food choice procedure. Psychopharmacology. 1991;104(4):515-21.
712 doi:10.1007/BF02245659.
713 42. Minamimoto T, Yamada H, Hori Y, Suhara T. Hydration level is an internal variable for computing
714 motivation to obtain water rewards in monkeys. Exp Brain Res. 2012;218(4):609-18. doi:
715 10.1007/s00221-012-3054-3.
716 43. Minamimoto T, Hori Y, Richmond BJ. Is working more costly than waiting in monkeys? PLoS
717 One. 2012;7(11):e48434. doi: 10.1371/journal.pone.0048434.
718 44. Kravitz AV, Freeze BS, Parker PRL, Kay K, Thwin MT, Deisseroth K, et al. Regulation of
719 parkinsonian motor behaviours by optogenetic control of basal ganglia circuitry. Nature.
720 2010;466(7306):622-U7. doi: 10.1038/nature09159.

721 45. Simmons JM, Minamimoto T, Murray EA, Richmond BJ. Selective ablations reveal that orbital
722 and lateral prefrontal cortex play different roles in estimating predicted reward value. J Neurosci.
723 2010;30(47):15878-87. doi:10.1523/jneurosci.1802-10.2010.
724 46. Callicott JH, Mattay VS, Bertolino A, Finn K, Coppola R, Frank JA, et al. Physiological
725 characteristics of capacity constraints in working memory as revealed by functional MRI. Cereb
726 Cortex. 1999;9(1):20-6. doi:10.1093/cercor/9.1.20.
727 47. Vijayraghavan S, Wang M, Birnbaum SG, Williams GV, Arnsten AFT. Inverted-U dopamine D1
728 receptor actions on prefrontal neurons engaged in working memory. Nat Neurosci.
729 2007;10(3):376-84. doi:10.1038/nn1846.
730 48. Richfield EK, Penney JB, Young AB. Anatomical and affinity state comparisons between
731 dopamine D1 and D2 receptors in the rat central nervous system. Neuroscience. 1989;30(3):767-
732 77. doi: 10.1016/0306-4522(89)90168-1.
733 49. Dreyer JK, Herrik KF, Berg RW, Hounsgaard JD. Influence of Phasic and Tonic Dopamine
734 Release on Receptor Activation. J Neurosci. 2010;30(42):14273-83. doi: 10.1523/jneurosci.1894-
735 10.2010.
736 50. Pardo M, Lopez-Cruz L, San Miguel N, Salamone JD, Correa M. Selection of sucrose
737 concentration depends on the effort required to obtain it: studies using tetrabenazine, D1, D2, and

738 D3 receptor antagonists. Psychopharmacology (Berl). 2015;232(13):2377-91. doi:
739 10.1007/s00213-015-3872-7.
740 51. Von Huben SN, Davis SA, Lay CC, Katner SN, Crean RD, Taffe MA. Differential contributions
741 of dopaminergic D1- and D2-like receptors to cognitive function in rhesus monkeys.
742 Psychopharmacology (Berl). 2006;188(4):586-96. doi: 10.1007/s00213-006-0347-x.
743 52. Wang S, Hu SH, Shi Y, Li BM. The roles of the anterior cingulate cortex and its dopamine
744 receptors in self-paced cost-benefit decision making in rats. Learn Behav. 2017;45(1):89-99. doi:
745 10.3758/s13420-016-0243-0.
746 53. Joutsa J, Voon V, Johansson J, Niemela S, Bergman J, Kaasinen V. Dopaminergic function and
747 intertemporal choice. Transl Psychiatry. 2015;5:e491. doi: 10.1038/tp.2014.133.
748 54. Pine A, Shiner T, Seymour B, Dolan RJ. Dopamine, time, and impulsivity in humans. J Neurosci.
749 2010;30(26):8888-96. doi: 10.1523/jneurosci.6028-09.2010.
750 55. Cardinal RN, Robbins TW, Everitt BJ. The effects of d-amphetamine, chlordiazepoxide, alpha-
751 flupenthixol and behavioural manipulations on choice of signalled and unsignalled delayed
752 reinforcement in rats. Psychopharmacology. 2000;152(4):362-75. doi:10.1007/s002130000536.
753 56. van Gaalen MM, van Koten R, Schoffelmeer ANM, Vanderschuren LJMJ. Critical involvement
754 of dopaminergic neurotransmission in impulsive decision making. Biol Psychiat. 2006;60(1):66-
755 73. doi: 10.1016/j.biopsych.2005.06.005.

756 57. Evenden JL, Ryan CN. The pharmacology of impulsive behaviour in rats: the effects of drugs on
757 response choice with varying delays of reinforcement. Psychopharmacology (Berl).
758 1996;128(2):161-70. doi: 10.1007/s002130050121.
759 58. Rajala AZ, Jenison RL, Populin LC. Decision making: effects of methylphenidate on temporal
760 discounting in nonhuman primates. J Neurophysiol. 2015;114(1):70-9. doi:
761 10.1152/jn.00278.2015.
762 59. Lak A, Stauffer WR, Schultz W. Dopamine prediction error responses integrate subjective value
763 from different reward dimensions. Proc Natl Acad Sci U S A. 2014;111(6):2343-8. doi:
764 10.1073/pnas.1321596111.
765 60. Pasquereau B, Turner RS. Limited encoding of effort by dopamine neurons in a cost-benefit trade-
766 off task. J Neurosci. 2013;33(19):8288-300. doi: 10.1523/jneurosci.4619-12.2013.
767 61. Gerfen CR, Surmeier DJ. Modulation of striatal projection systems by dopamine. Annu Rev
768 Neurosci. 2011;34:441-66. doi: 10.1146/annurev-neuro-061010-113641.
769 62. Hikida T, Kimura K, Wada N, Funabiki K, Nakanishi S. Distinct roles of synaptic transmission in
770 direct and indirect striatal pathways to reward and aversive behavior. Neuron. 2010;66(6):896-
771 907. doi: 10.1016/j.neuron.2010.05.011.

772 63. Kupchik YM, Brown RM, Heinsbroek JA, Lobo MK, Schwartz DJ, Kalivas PW. Coding the
773 direct/indirect pathways by D1 and D2 receptors is not valid for accumbens projections. Nat
774 Neurosci. 2015;18(9):1230-2. doi: 10.1038/nn.4068.
775 64. Lee B, Groman S, London ED, Jentsch JD. Dopamine D2/D3 receptors play a specific role in the
776 reversal of a learned visual discrimination in monkeys. Neuropsychopharmacology.
777 2007;32(10):2125-34. doi: 10.1038/sj.npp.1301337.
778 65. Nagai Y, Minamimoto T, Ando K, Obayashi S, Ito H, Ito N, et al. Correlation between decreased
779 motor activity and dopaminergic degeneration in the ventrolateral putamen in monkeys receiving
780 repeated MPTP administrations: a positron emission tomography study. Neurosci Res.
781 2012;73(1):61-7. doi: 10.1016/j.neures.2012.02.007.
782 66. Gunn RN, Lammertsma AA, Hume SP, Cunningham VJ. Parametric imaging of ligand-receptor
783 binding in PET using a simplified reference region model. Neuroimage. 1997;6(4):279-87. doi:
784 10.1006/nimg.1997.0303.
785 67. Jucaite A, Odano I, Olsson H, Pauli S, Halldin C, Farde L. Quantitative analyses of regional
786 [11C]PE2I binding to the dopamine transporter in the human brain: a PET study. Eur J Nucl Med
787 Mol Imaging. 2006;33(6):657-68. doi: 10.1007/s00259-005-0027-9.
788 68. Lammertsma AA, Hume SP. Simplified reference tissue model for PET receptor studies.
789 Neuroimage. 1996;4(3 Pt 1):153-8. doi: 10.1006/nimg.1996.0066.

790 69. Cunningham VJ, Rabiner EA, Slifstein M, Laruelle M, Gunn RN. Measuring drug occupancy in
791 the absence of a reference region: the Lassen plot re-visited. J Cereb Blood Flow Metab.
792 2010;30(1):46-50. doi: 10.1038/jcbfm.2009.190.
793 70. Bates D, Mächler M, Bolker B, Walker S. Fitting Linear Mixed-Effects Models Using lme4.
794 Journal of Statistical Software. 2015;67(1):1-48. doi: 10.18637/jss.v067.i01.

795 **Supporting information**

796 **S1 Table. Model comparison.** *a(cond)* and *e(cond)* indicate the random effects of DAR blocking
797 treatment conditions on parameters *a* and *e*, respectively. AIC (Akaike's information criterion) is a
798 relative measure of quality for the models (#1-4). ΔAIC denotes difference from minimum AIC.

799

800 **S1 Fig. Occupancy estimation.** Example of occupancy estimation based on modified Lassen plot of
801 [^{11}C]SCH23390 PET data obtained from monkey DO. Colored dots represent the relationship between
802 decreased specific binding [i.e., BP_{ND} (baseline) – BP_{ND} (blocking)] and baseline [BP_{ND} (baseline)]
803 for each brain region under each blocking condition (indexed by color). Occupancy was determined
804 as a proportion of reduced specific binding to baseline, which corresponds to the slope of linear
805 regression. In this case, D_1 occupancy was 80%, 78%, 67%, and 26% for 100, 50, 30 and 10 μg/kg
806 doses, respectively.

807

808 **S2 Fig. Comparable effects of D_2R antagonism between raclopride and haloperidol at similar**
809 **occupancy.** (A) Occupancy of D_2R measured at striatal ROI is plotted against dose of raclopride. (B)
810 Error rates as a function of reward size for control (black) and after injection of raclopride (10 μg/kg,
811 i.m, left side) and haloperidol (10 μg/kg, i.m, right side) in monkey KN are plotted. Dotted curves are
812 best-fit inverse function (*model #1* in S1 Table).

S3 Fig. Effect of D_1R/D_2R blockade on reaction time and error pattern. (A-B) Mean reaction time as function of reward size for control and D_1R blockade conditions. (C-D) Late release rate (mean ± SEM) as function of reward size for control and D_1R blockade conditions. (E-H) Same as (A-D), but for D_2R blockade. Data were obtained from monkey ST.

S4 Fig. Little influence of DAR blockades on sucrose preference and blood osmolality. (A) Sucrose preference index after administration of saline (Control), SCH23390 (30μg/kg, D_1), and haloperidol (10μg/kg; D_2, day 0), respectively. (B) Blood osmolality measured in serum samples obtained before (Pre) and after (Post) sucrose test. Filled circles and shades indicate median and raw data points, while horizontal bars indicate SD.

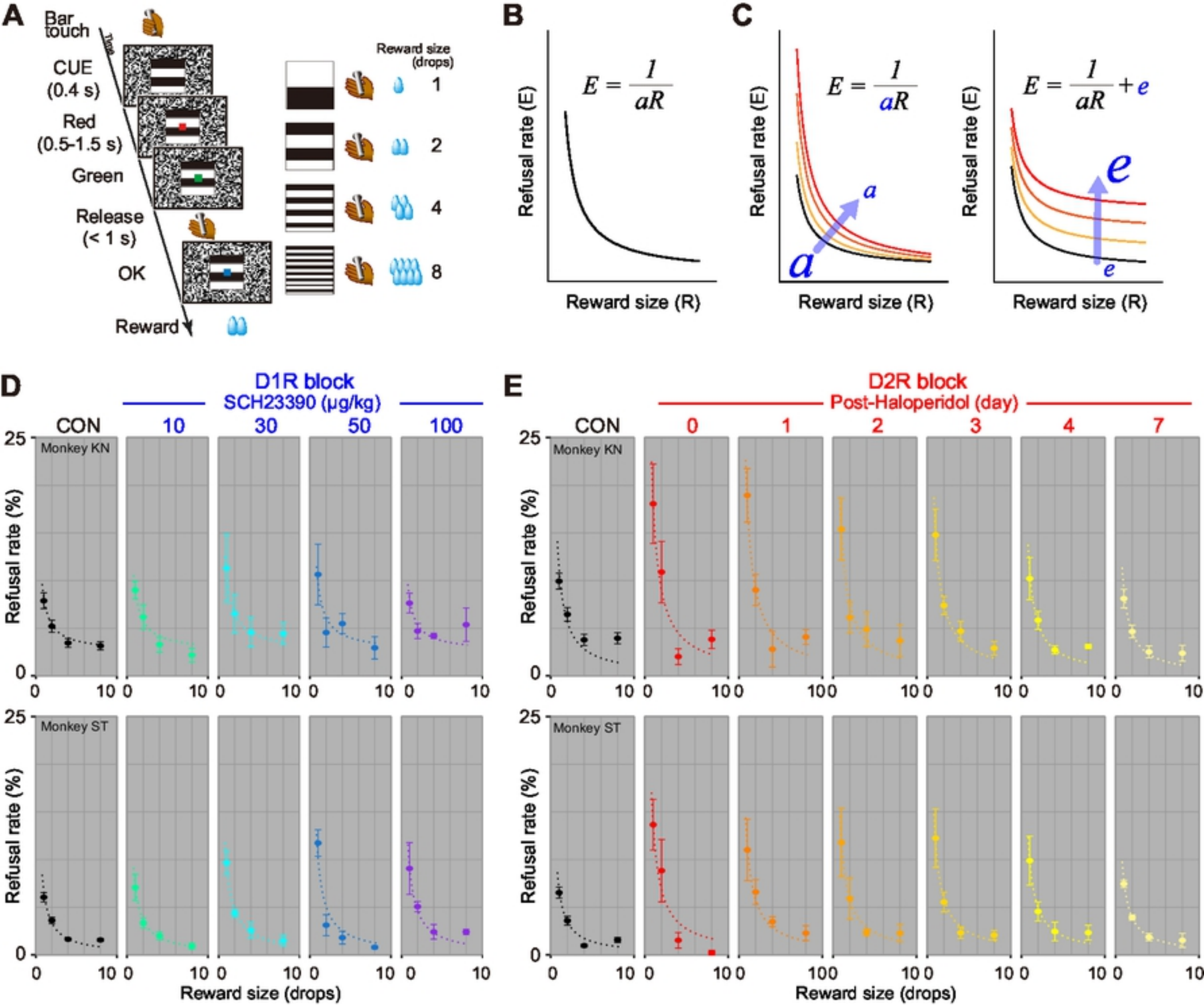
A
Bar touch
Time
CUE (0.4 s)
Red (0.5-1.5 s)
Green
Release (< 1 s)
OK
Reward
Reward size (drops)
1
2
4
8
B
Refusal rate (E)
$E = \frac{1}{aR}$
Reward size (R)
C
Refusal rate (E)
$E = \frac{1}{aR}$
a
Reward size (R)
$E = \frac{1}{aR} + e$
e
Reward size (R)
D
D1R block
SCH23390 (μg/kg)
CON
10
30
50
100
Monkey KN
Monkey ST
Refusal rate (%)
Reward size (drops)
E
D2R block
Post-Haloperidol (day)
CON
0
1
2
3
4
7
Monkey KN
Monkey ST
Refusal rate (%)
Reward size (drops)

Figure2

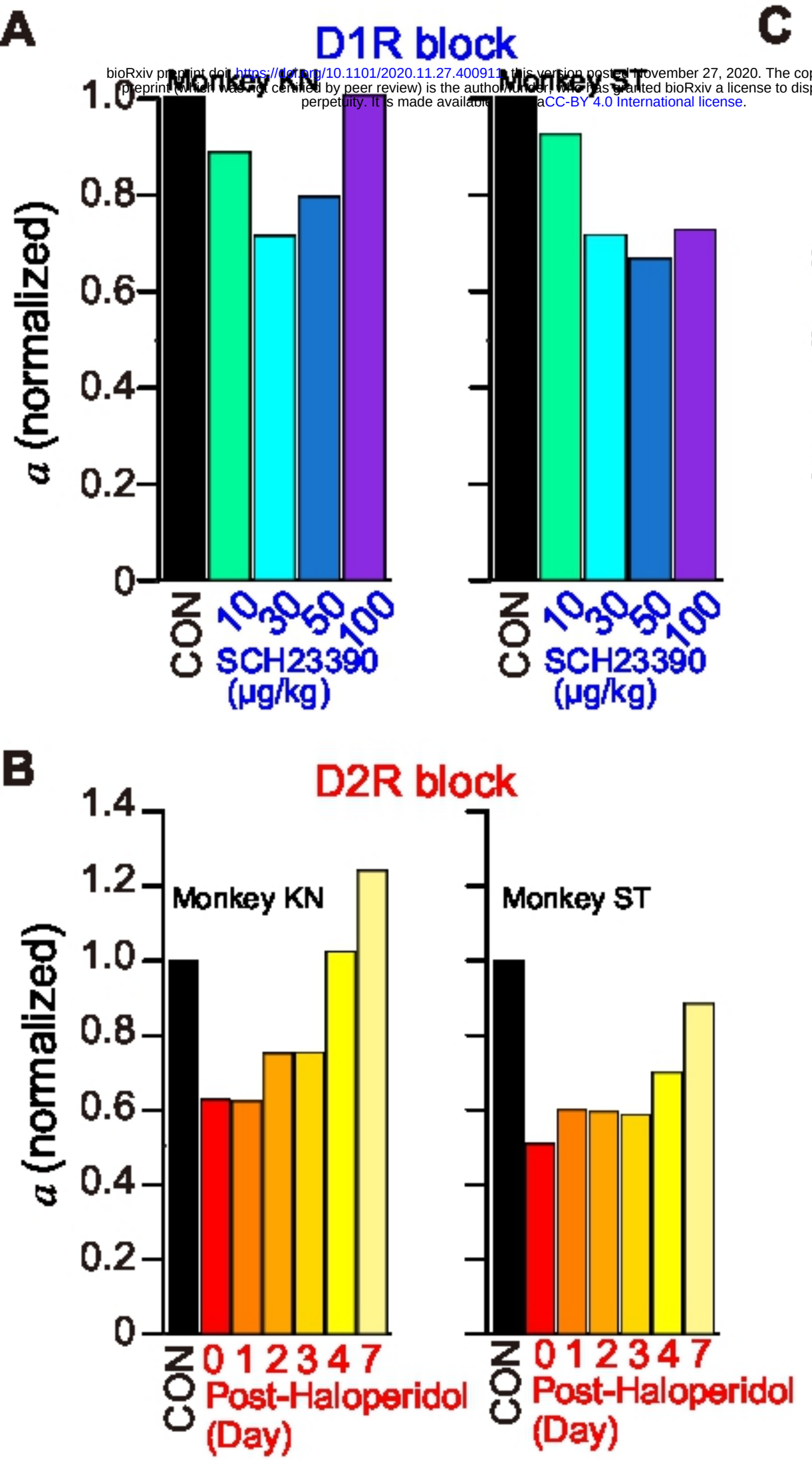

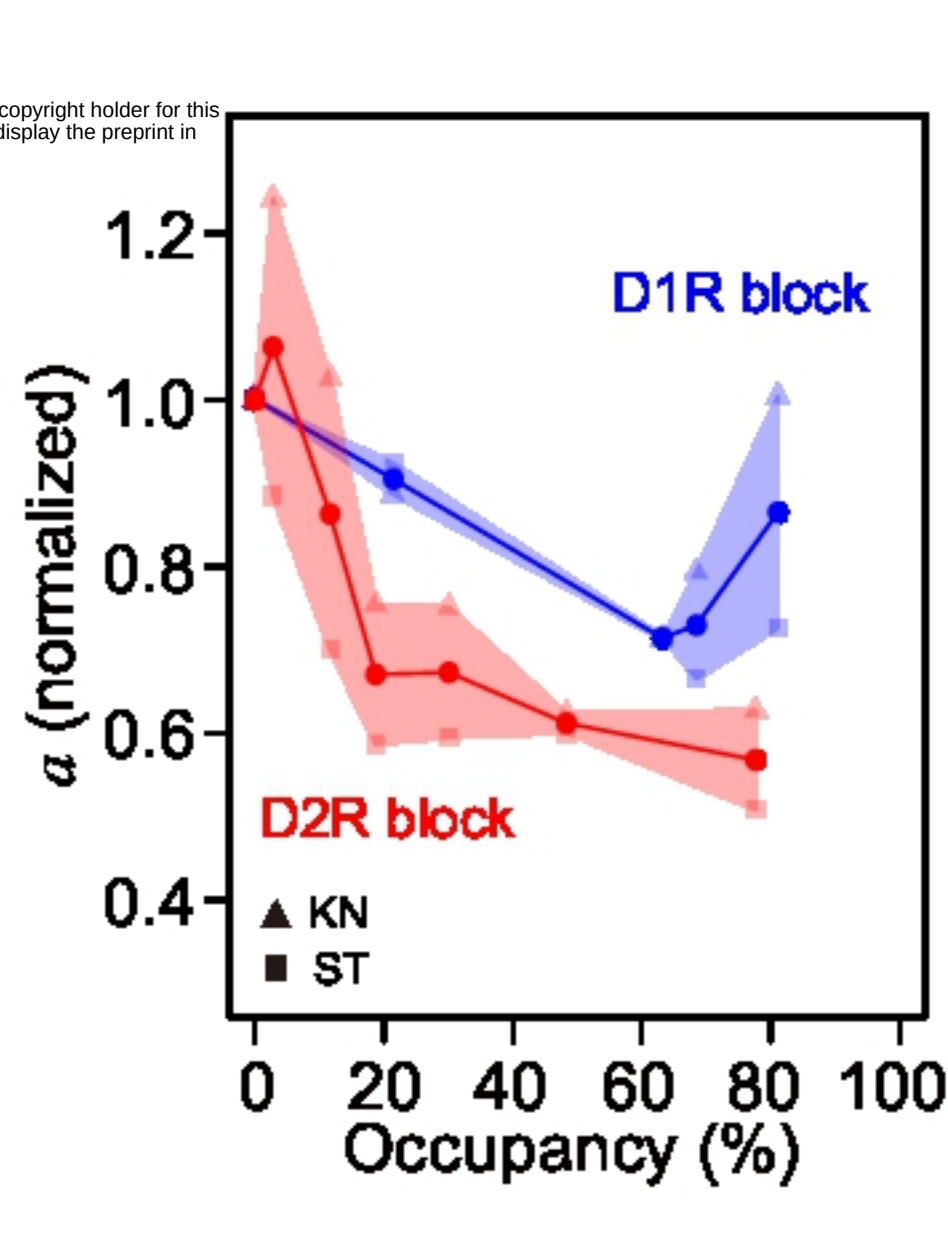

Figure3

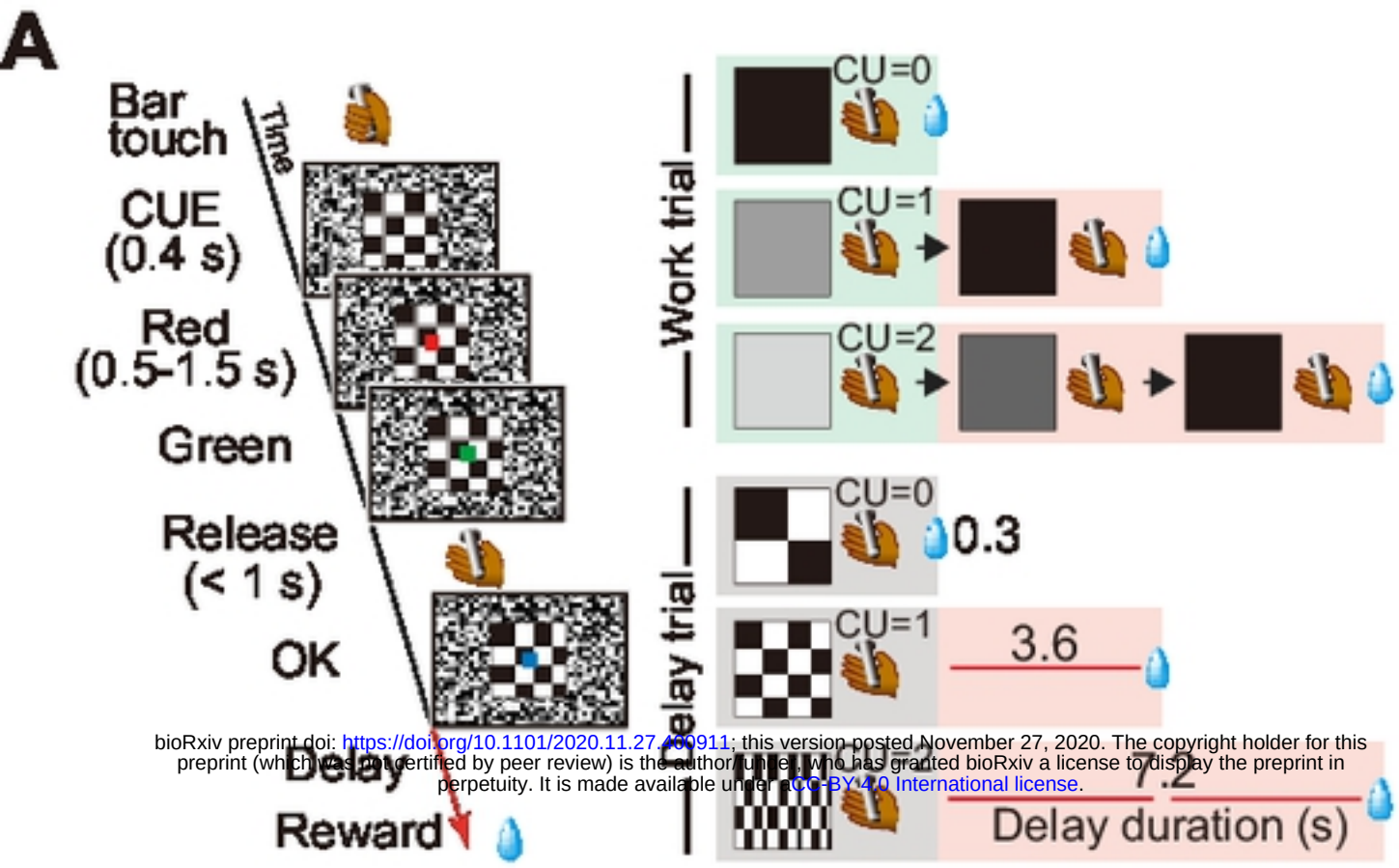

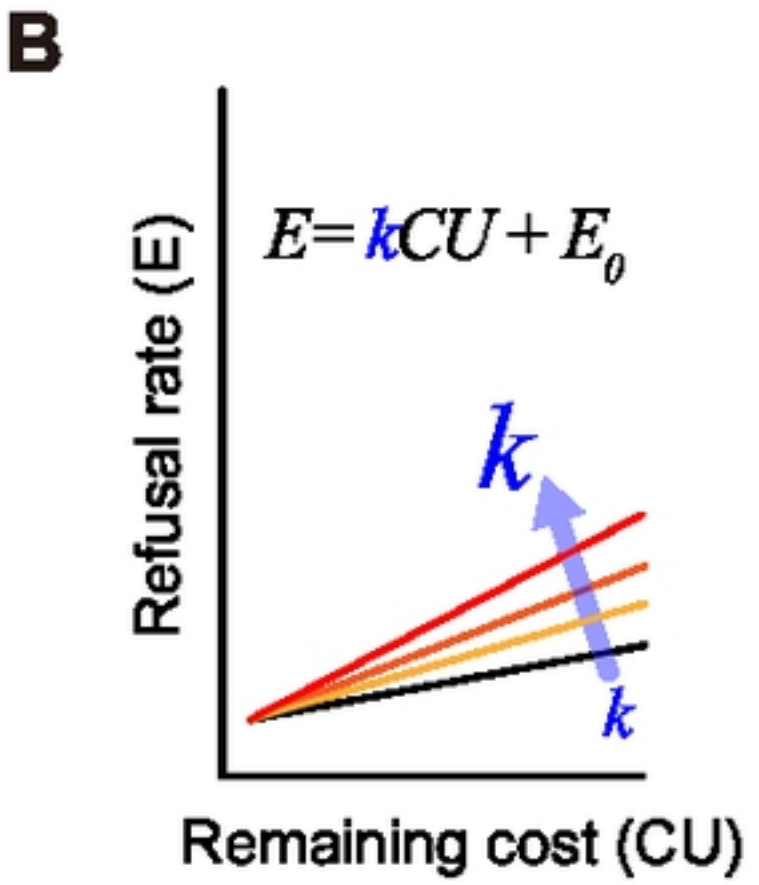

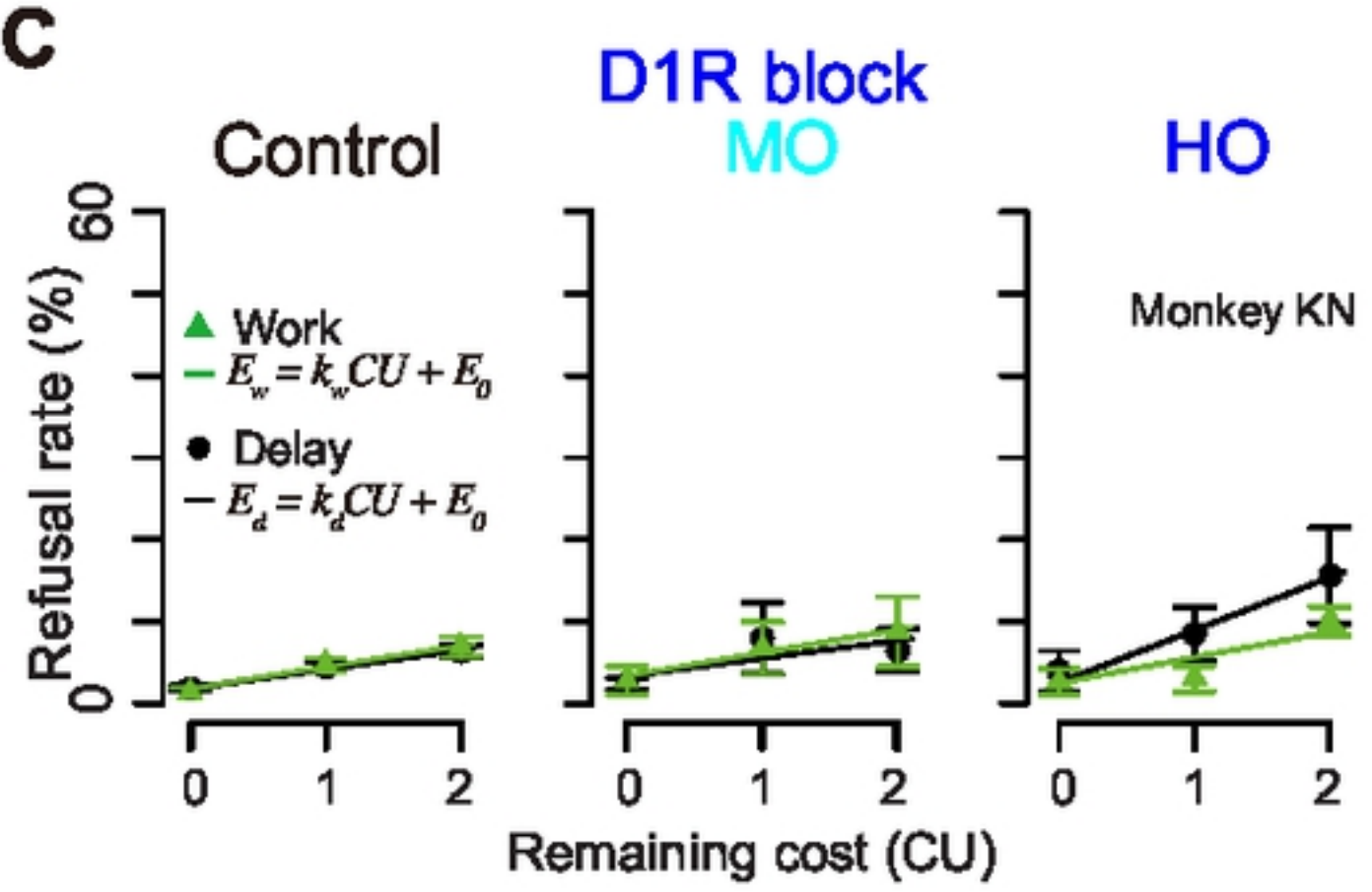

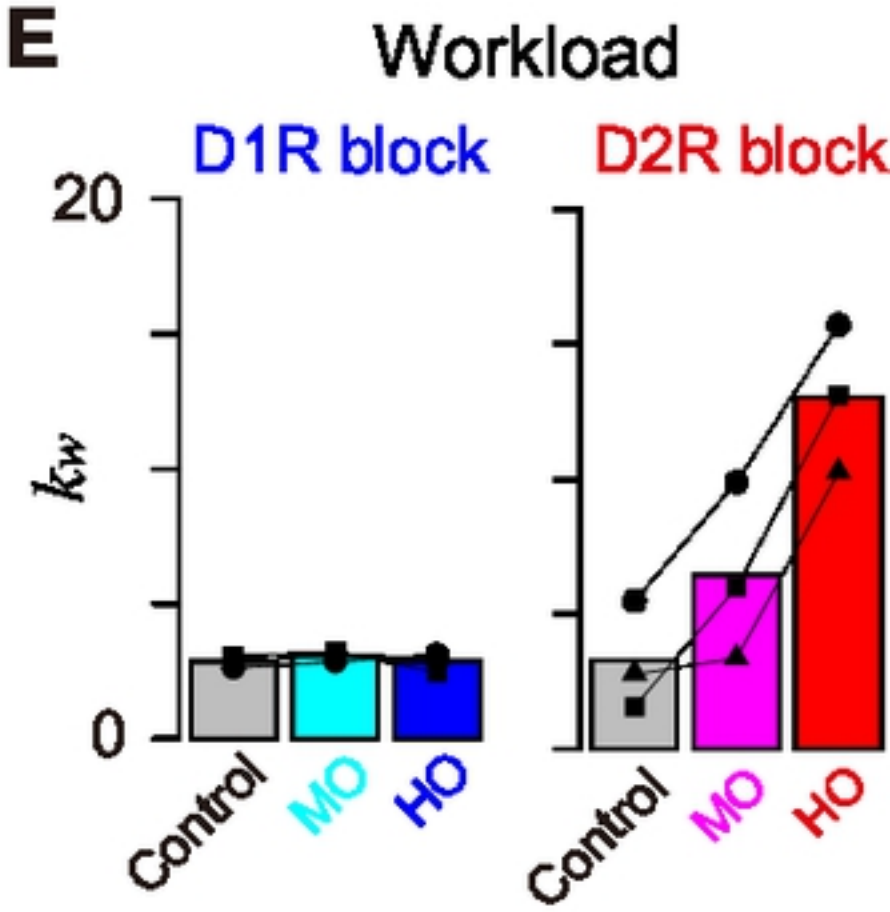

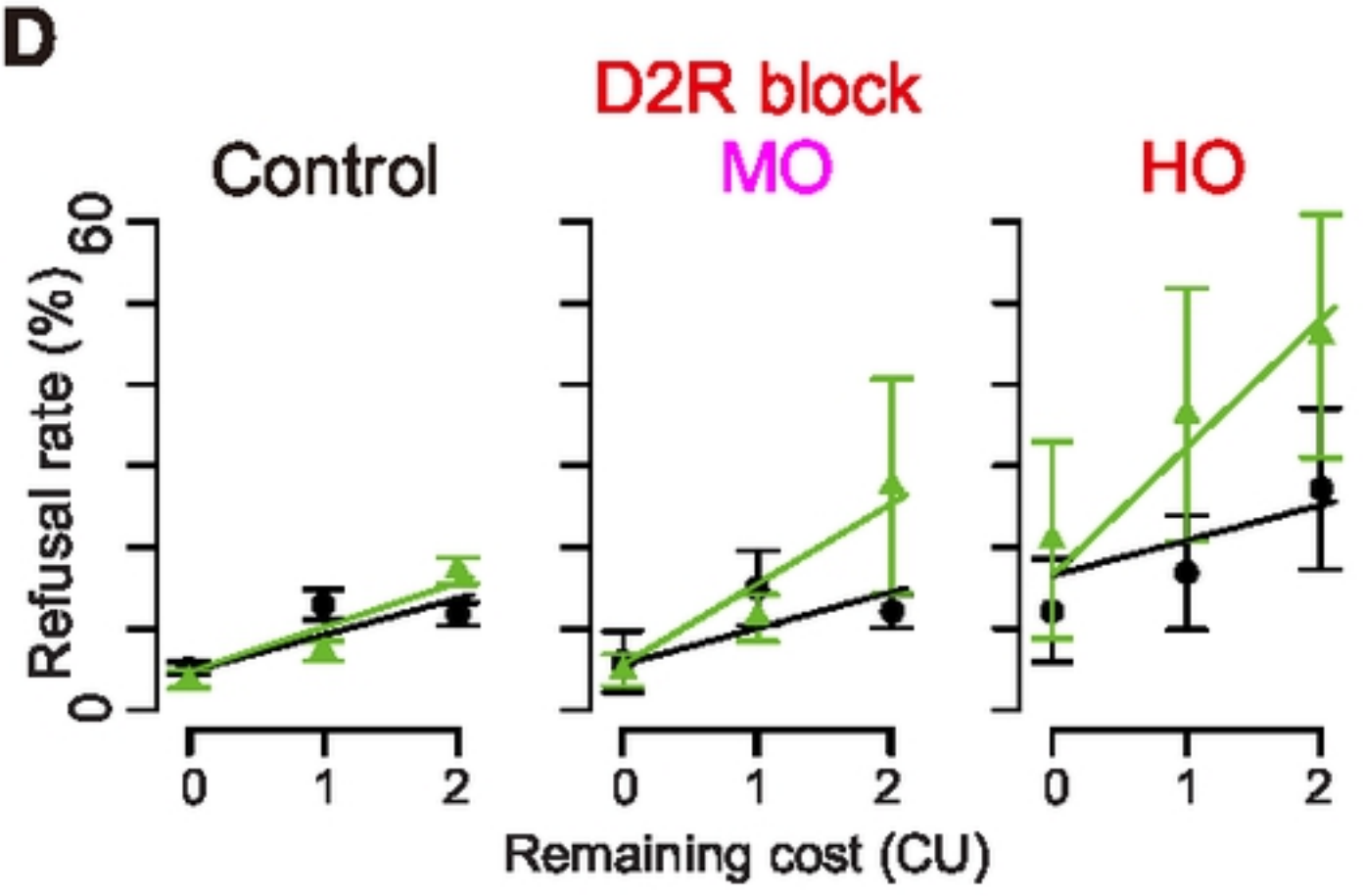

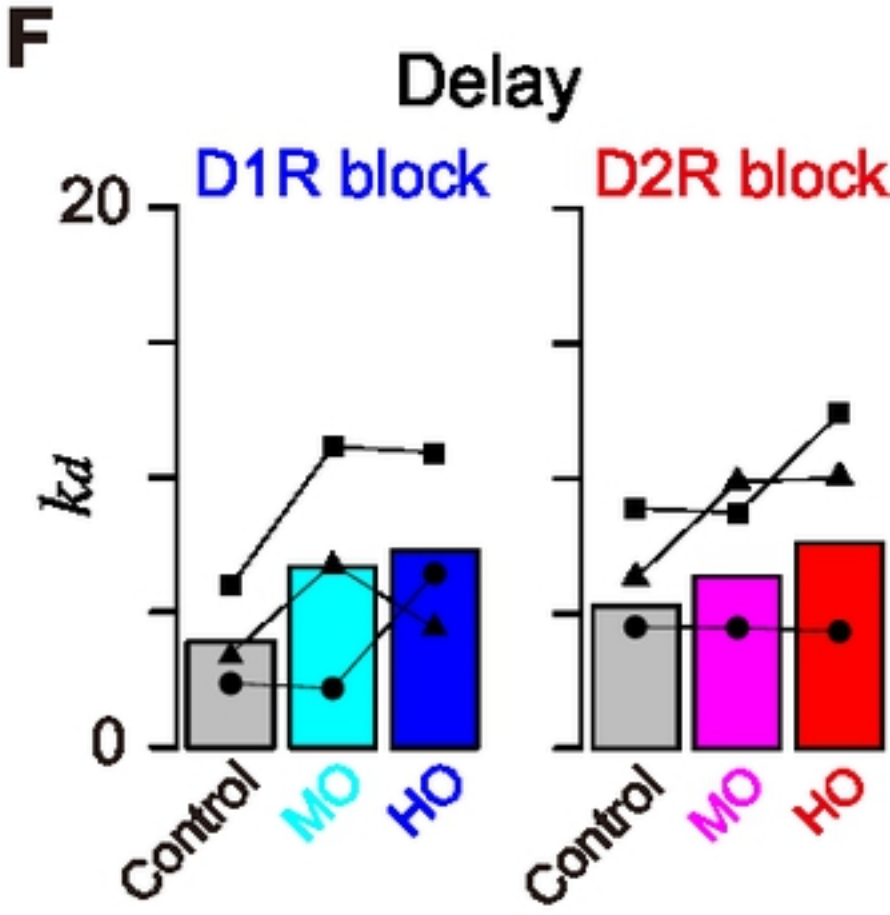

Figure4

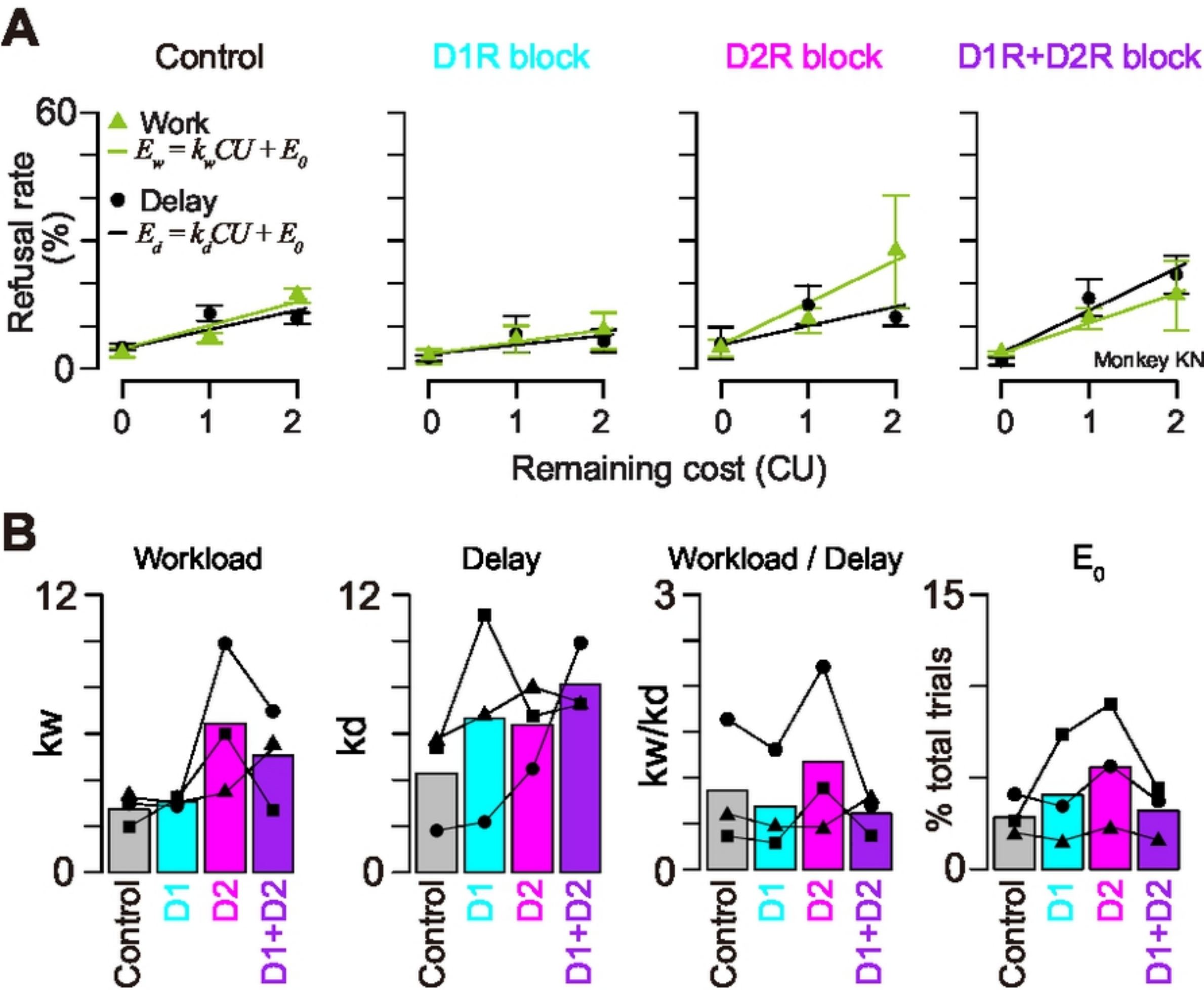
A
Control
D1R block
D2R block
D1R+D2R block
60
0
Refusal rate (%)
Work
$E_w = k_w CU + E_0$
Delay
$E_d = k_d CU + E_0$
0
1
2
Monkey KN
Remaining cost (CU)
B
Workload
Delay
Workload / Delay
E_0
12
0
kw
kd
3
kw/kd
15
% total trials
Control
D1
D2
D1+D2

Figure5

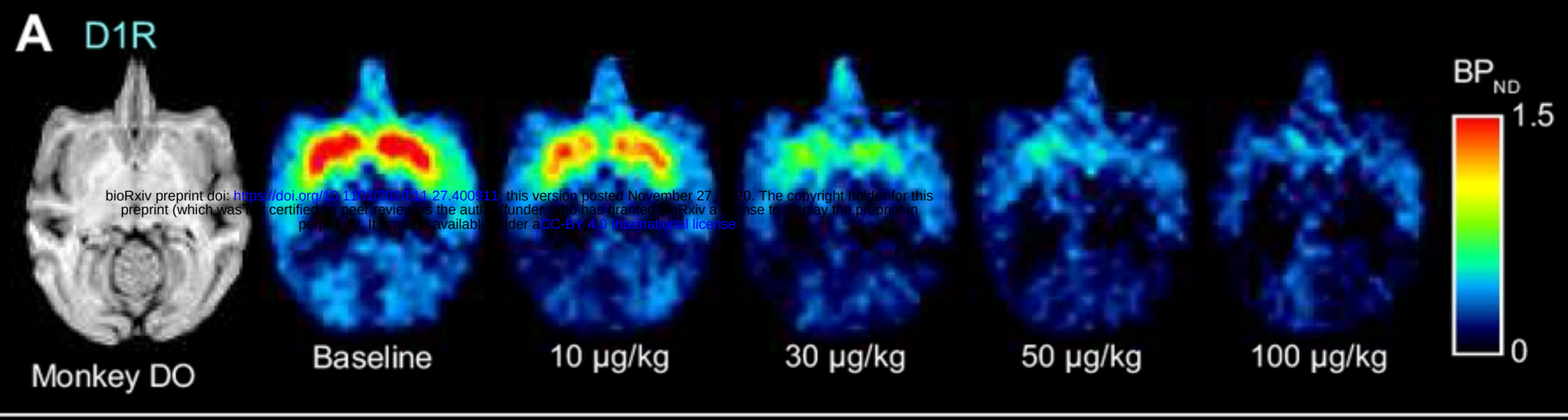

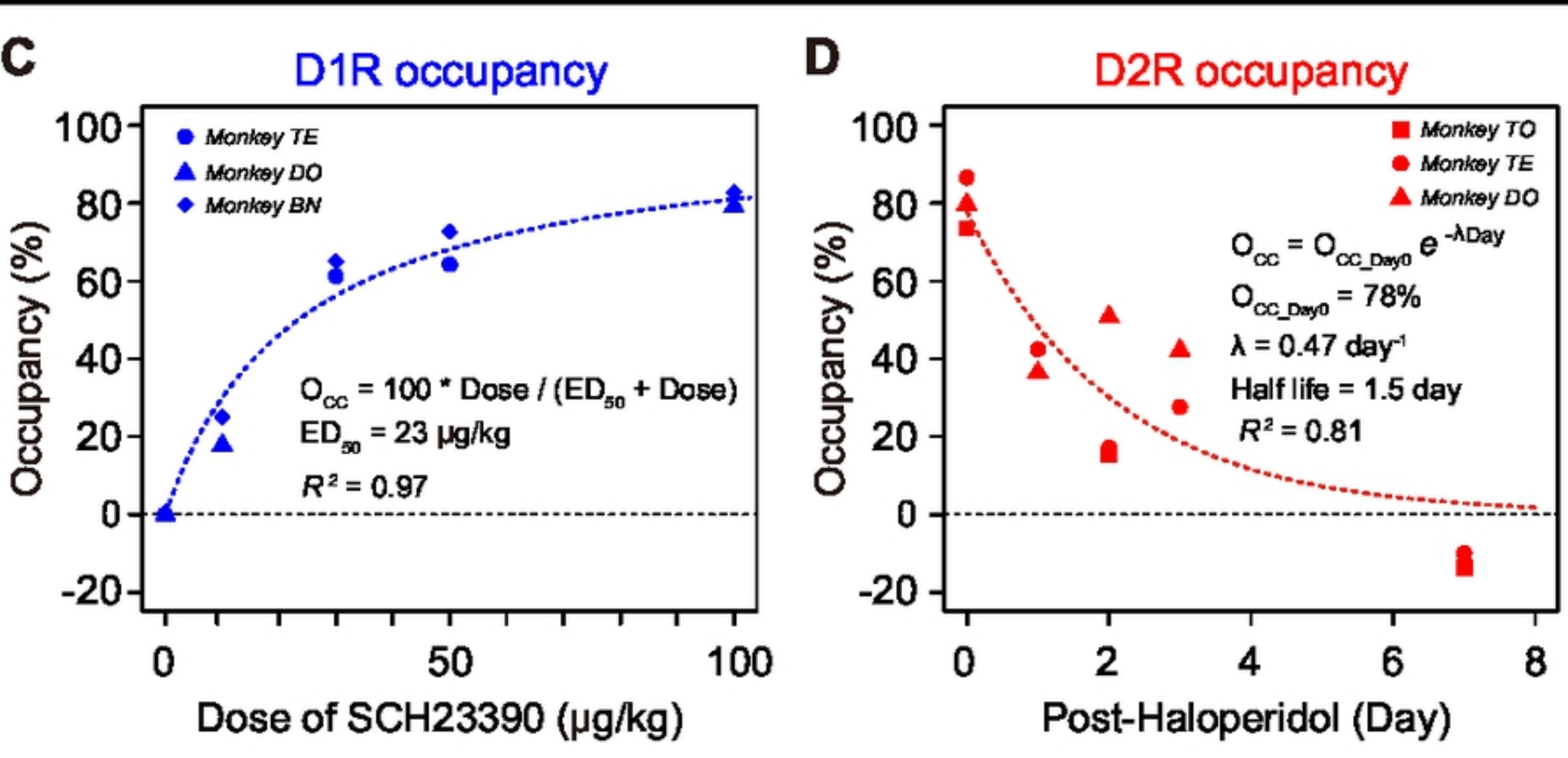

Figure1